Discovery of biased orientations of human regulatory motifs affecting transcription of genes and including known insulators

Naoki Osato[1*]

[1]Department of Bioinformatic Engineering, Graduate School of Information Science and Technology, Osaka University, Osaka 565-0871, Japan

[*]Corresponding author

E-mail address: naokiosato11@gmail.com, nosato@ist.osaka-u.ac.jp

Abstract

Chromatin interactions play essential roles in enhancer-promoter interactions (EPIs) and regulating the transcription of genes. CTCF and cohesin proteins are located at the anchors of chromatin interactions, forming their loop structures. Other DNA binding proteins such as YY1, ZNF143 and SMARCA4 are also reported to be involved in chromatin interactions. However, the overall picture of proteins associated with chromatin interactions and insulator function is still unclear. Here I describe a systematic and comprehensive approach to discover DNA binding motif sequences of transcription factors (TFs), affecting the interaction between enhancers and promoters of genes and their expression by the insulator function of the TFs. This analysis identified 96 biased orientations of DNA motifs of TFs that affected the expression level of putative transcriptional target genes significantly in monocytes, T cells, HMEC and NPC in common, and included known TFs involved in chromatin interaction and insulator function such as CTCF, cohesin (RAD21 and SMC3), YY1 and ZNF143. The 96 biased orientations of DNA motifs contain 64 forward-reverse (FR) and 52 reverse-forward (RF) orientations of DNA motifs (Some TFs have more than one DNA motifs in databases, so the total number is smaller than the sum of FR and RF). To confirm the predicted DNA motifs, first, I compared with chromatin interaction data. Despite the limitation of resolution of chromatin interaction data, for 44 (69%) FR and 28 (54%) RF orientations of DNA motif sequences in $CD4^+$ T cells, EPIs predicted based on an enhancer-promoter association (EPA) that was shortened at the biased orientations of DNA motif sites, overlapped with chromatin interactions significantly

more than other types of EPAs. Second, using gene expression data among 53 tissues, 43 (72%) FR and 40 (80%) RF orientations of DNA motifs showed a significantly reduced correlation in expression level of nearby genes separated by the motif sites. Some DNA motif sites of biased orientations of DNA motifs of TFs were found between nearby genes not including DNA motif sites of the known TFs involved in chromatin interactions and between a low correlation of expression level of nearby genes. These analyses suggest that the DNA motifs are associated with insulator functions.

Keywords: transcriptional target genes, gene expression, transcription factors, enhancer, enhancer-promoter interactions, chromatin interactions, CTCF, cohesin, open chromatin regions, co-location of transcription factors, homodimer, heterodimer, complex

Background

Chromatin interactions play essential roles in enhancer-promoter interactions (EPIs) and regulating the transcription of genes. CTCF and cohesin proteins are located at the anchors of chromatin interactions, forming their loop structures. CTCF has insulator function limiting the activity of enhancers into the loops (Fig. 1A). The DNA binding sequence of CTCF indicate its orientation bias at chromatin interaction anchors – forward-reverse (FR) orientation is frequently observed (Rao et al. 2014; de Wit et al. 2015; Guo et al. 2015). Other DNA binding proteins such as ZNF143, YY1 and SMARCA4 (BRG1) are involved in chromatin interaction and EPI (Bailey et al. 2015;

55 Barutcu et al. 2016; Weintraub et al. 2017). ZNF143 is known to bind more to promoter
56 of genes than distal regions, establishing looping with distal element bound by CTCF
57 (Bailey et al. 2015). DNA binding motif sequence of ZNF143 is significantly enriched
58 at both chromatin interaction anchors (Z-score > 7), whereas DNA binding motif
59 sequence of YY1 does not seem to be enriched (Z-score < 2; Bailey et al. 2015 Figure
60 2a). CTCF, cohesin, ZNF143, YY1 and SMARCA4 have various biological functions
61 other than chromatin interaction. These transcription factors (TFs) are bound in open
62 chromatin regions near transcriptional start sites (TSS) as well as chromatin interaction
63 anchors, which may reduce the enrichment of the DNA motif sites of the TFs at
64 chromatin interaction anchors.

65 Computational approaches to predict chromatin interactions were developed
66 (Schreiber et al. 2017; Zhang et al. 2017). However, they were not intended to find
67 DNA motif sequences of TFs involved in chromatin interactions. (Xie et al. 2005)
68 mentioned in Conclusion section that the next challenge will be to develop systematic
69 methods to discern the specific functions of these motifs in a genome-wide fashion.

70 DNA binding proteins involved in chromatin interactions are considered to affect
71 the transcription of genes in the loops formed by chromatin interactions. To confirm this
72 notion, I previously found that the expression level of human putative transcriptional
73 target genes of a TF was significantly changed, according to the criteria of
74 enhancer-promoter association (EPA) (Osato 2018). An EPA was shortened at the FR
75 orientation of CTCF binding sites, and transcriptional target genes of each TF bound in
76 enhancers and promoters were predicted based on the EPA (Fig. 1B). The expression

77 levels of the transcriptional target genes were significantly different, compared with the
78 expression levels of transcriptional target genes of TFs predicted based on only
79 promoters (or closed chromatin regions). The expression levels tend to be increased in
80 monocytes and $CD4^+$ T cells, implying that enhancers activate the transcription of genes.
81 The expression levels tend to be decreased in ES and iPS cells, implying that enhancers
82 repress the transcription of genes. The expression level of putative transcriptional target
83 genes of a TF bound in enhancers is changed significantly, when EPIs are predicted
84 properly using the insulator sites of CTCF in cell types. This suggests that the difference
85 of the expression level would reflect the accuracy of prediction of transcriptional target
86 genes of a TF based on a given EPA. Using this approach, I planned to search for other
87 DNA binding proteins involved in chromatin interactions, affecting the expression level
88 of putative transcriptional target genes through their insulator function.

89 Experimental analyses of chromatin interactions in molecular biology have
90 technical limitations: chromatin interaction data are altered, according to experimental
91 techniques, the number of reads of DNA sequencing and even replication sets of the
92 same cell type. Chromatin interaction data may not be saturated enough to contain all
93 chromatin interactions and may include experimental noises such as ligation error.
94 Avoiding the technical limitations of experimental analyses, here I searched
95 computationally for DNA motif sequences of TFs, affecting EPI and the expression
96 level of putative transcriptional target genes in monocytes, T cells, HMEC and NPC
97 without using chromatin interaction data. Then, putative EPIs and DNA motif sites of
98 TFs were compared with chromatin interaction and gene expression data.

99

100 ## Results

101 **Search for biased orientations of DNA motif sequences**

102 Transcription factor binding sites (TFBSs) were predicted using open chromatin
103 regions and DNA motif sequences of transcription factors (TF) collected from various
104 databases and journal papers (see Methods). Transcriptional target genes were predicted
105 based on TFBS in promoters and enhancers. An enhancer-promoter association (EPA)
106 was shortened at the DNA binding motif sites of a TF acting as insulator such as CTCF
107 and cohesin (RAD21 and SMC3) (Fig. 1B). To find DNA motif sequences of TFs with
108 insulator function, other than CTCF and cohesin, affecting the expression level of genes,
109 An EPA was shortened at the DNA motif sites of a putative insulator TF, and
110 transcriptional target genes of each general TF bound in (i) distal open chromatin
111 regions (enhancers) and (ii) closed chromatin regions in promoters were predicted based
112 on the EPA, in order to estimate the enhancer activity of each general TF. The ratio of
113 expression level of putative transcriptional target genes of each TF between (i) and (ii)
114 was calculated. The distribution of the ratios of all general TFs was compared among
115 forward-reverse (FR), reverse-forward (RF) orientations and non-orientation (i.e.
116 without considering orientation) of DNA motif sites of an insulator TF shortening an
117 EPA using Mann-Whitney test, two-sided (p-value $< 10^{-7}$), and putative insulator TFs
118 with significant differences of the distributions of the ratios of expression level among
119 FR, RF orientations and non-orientation were enumerated (Fig. 2A).

120 To confirm the prediction of TFBS, the distributions of TFBS were examined in

121 the human genome. TFBS involved in chromatin interactions were identified near TSS
122 (Fig. 2B). ZNF143 is known to bind to promoter of genes establishing looping with
123 distal element bound by CTCF (Fig. 5) (Bailey et al. 2015). YY1 is multi-functional
124 transcriptional regulator and is involved in transcriptional activation, repression and
125 initiation (Shrivastava and Calame 1994; Xi et al. 2007). Most of DNA motif sites of
126 the TFs were identified in intergenic and intron regions of the human genome (Fig. 2C).

127 Several hundreds of FR and RF orientations of DNA motifs of TFs were found in
128 monocytes, T cells, human mammary epithelial cells (HMEC) and neural progenitor
129 cells (NPC) (Fig. 3). The number of the TFs seemed to be changed, according to the
130 number of DNase-seq reads, since the number of the reads in monocyte is larger than
131 the other three cell types. When DNase-seq reads increase, more TFBS may be
132 predicted to some extent. Total 96 of biased (64 FR and 52 RF) orientations of DNA
133 binding motif sequences of TFs were discovered in the four cell types in common,
134 whereas non-orientation of DNA binding motif sequences of TFs were not detected (Fig.
135 3; Table 1; Supplemental material). The FR orientation of DNA motif sequences
136 included CTCF, cohesin (RAD21 and SMC3), YY1 and ZNF143, which are involved in
137 chromatin interaction and EPI.

138 Without considering the difference of orientations of DNA binding motif
139 sequences among cell types, 175 biased orientations of DNA binding motif sequences
140 of TFs were found in the four cell types in common. These numbers (96 and 175) are
141 unique numbers of TFs with biased orientations of DNA motifs, and not the unique
142 numbers of DNA motifs. Possible causes of the number 175 increased from 96 are as

143 follows: (1) a TF or an isoform of the same TF may bind to a different DNA binding
144 motif sequence, according to cell types and/or in the same cell type. About 50% or more
145 of alternative splicing isoforms are differently expressed among tissues, indicating that
146 most alternative splicing is subject to tissue-specific regulation (Das et al. 2007; Wang
147 et al. 2008; Chen and Manley 2009). (2) The same TF has several DNA binding motif
148 sequences, and in some cases one of the motif sequences is almost the same as the
149 reverse complement sequence of another motif sequence of the same TF in the same or
150 different databases of TFs. (3) I previously found that a complex of TFs would bind to a
151 slightly different DNA binding motif sequence from the combination of DNA binding
152 motif sequences of TFs composing the complex in *C. elegans* (Tabuchi et al. 2011). In
153 other reports, the difference of binding specificity of pairs of TFs was investigated
154 (Jolma et al. 2015). Cofactors also contribute to alter binding specificity of TFs (Ansari
155 and Peterson-Kaufman 2011; Slattery et al. 2011; Merabet and Mann 2016). These
156 increase the variety and number of (biased orientations of) DNA binding motif
157 sequences of a TF, which are potentially involved in different biological functions
158 among cell types.
159
160 **Comparison with chromatin interaction data**
161 To ask whether the biased orientations of DNA motif sequences are associated
162 with chromatin interaction, enhancer-promoter interactions (EPIs) predicted based on an
163 enhancer-promoter association (EPA) were compared with chromatin interaction data.
164 EPIs predicted based on an EPA were compared with three replications (B2T1, B2T2

165 and B3T1) of HiChIP chromatin interaction data in $CD4^+$ T cells separately (Mumbach
166 et al. 2017). The resolutions of HiChIP chromatin interaction data and EPIs were
167 adjusted to 5 kilobases (kb). The number of unique HiChIP cis (i.e. in the same
168 chromatin) chromatin interactions was 19,926,360 at 5 kb resolution in B2T1
169 replication of T cells, 666,149 at 5 kb resolution with ≥1,000 counts for each
170 interaction and 78,209 at 5 kb resolution with ≥6,000 counts for each interaction
171 (Supplemental material). EPI were predicted based on three types of EPAs: (i) EPA
172 shortened at the FR or RF orientation of DNA motif sites of a TF with putative insulator
173 function such as CTCF, (ii) EPA shortened at the DNA motif sites of a TF without
174 considering their orientation, and (iii) EPA without being shortened by DNA motif sites.
175 For total 201 biased orientations [133 (49%) FR and 90 (43%) RF of 273 FR and 211
176 RF] of DNA motif sequences in T cells, which included CTCF, cohesin (RAD21 and
177 SMC3), ZNF143 and YY1 in three replications (B2T1, B2T2, and B3T1), a
178 significantly higher ratio of EPIs overlapped with HiChIP chromatin interactions with
179 ≥1,000 counts for each interaction in EPA (i) than the other types of EPA (ii) and (iii) in
180 T cells (Table 2). When comparing EPIs predicted based on only EPA (i) and (iii) with
181 the chromatin interactions, for total 390 biased orientations [261 (96%) FR and 199
182 (94%) RF of 273 FR and 211 RF] of DNA motif sequences in T cells, a significantly
183 higher ratio of EPIs overlapped with the chromatin interactions in EPA (i) than EPA (iii)
184 (Table 2; Supplemental material). The difference between EPIs predicted based on EPA
185 (i) and (ii) seemed to be difficult to distinguish using the chromatin interaction data and
186 a statistical test in some cases. However, as for the difference between EPIs predicted

187 based on EPA (i) and (iii), a larger number of biased orientations of DNA motif
188 sequences were correlated with chromatin interaction data. Most of biased orientations
189 of DNA motif sequences (95%) were correlated with chromatin interactions, when
190 comparing EPIs predicted based on EPA (i) and (iii) with HiChIP chromatin interactions.
191 Chromatin interaction data were obtained from different samples from DNase-seq open
192 chromatin regions, so individual differences may exist. Individual differences of
193 chromatin interactions were larger than those of open chromatin regions (Mumbach et
194 al. 2017).

195 Additionally, to confirm these tendencies of comparison of EPIs with HiChIP
196 chromatin interactions, the same analysis was conducted using HiChIP chromatin
197 interaction data in Th17, Treg and GM12878 cells. For total 128 biased orientations [76
198 (38%) FR and 64 (35%) RF of 200 FR and 183 RF] of DNA motif sequences in Th17
199 cells, which included CTCF, cohesin (RAD21 and SMC3), ZNF143 and YY1 in three
200 replications (B1T2, B2T1, and B3T1), a significantly higher ratio of EPIs overlapped
201 with HiChIP chromatin interactions in EPA (i) than the other types of EPA (ii) and (iii)
202 (Supplemental material). When comparing EPIs predicted based on only EPA (i) and
203 (iii) with the chromatin interactions, for total 282 biased orientations [182 (91%) FR
204 and 162 (89%) RF of 200 FR and 183 RF] of DNA motif sequences, a significantly
205 higher ratio of EPIs overlapped with the chromatin interactions in EPA (i) than EPA (iii)
206 (Supplemental material).

207 In Treg cells, chromatin interactions in one biological replication were overlapped
208 with EPIs, but those in the other two biological replications were less overlapped with

209 EPIs, so the one replication (B3T1) was used for this analysis. For total 281 biased
210 orientations [154 (53%) FR and 176 (54%) RF of 290 FR and 323 RF] of DNA motif
211 sequences, which included CTCF, cohesin (RAD21 and SMC3), ZNF143 and YY1, a
212 significantly higher ratio of EPIs overlapped with HiChIP chromatin interactions in EPA
213 (i) than the other types of EPA (ii) and (iii) (Supplemental material). When comparing
214 EPIs predicted based on only EPA (i) and (iii) with the chromatin interactions, for total
215 482 biased orientations [283 (98%) FR and 309 (96%) RF of 290 FR and 323 RF] of
216 DNA motif sequences, a significantly higher ratio of EPIs overlapped with the
217 chromatin interactions in EPA (i) than EPA (iii) (Supplemental material).

218 In GM12878 cells, for total 168 biased orientations [96 (38%) FR and 98 (35%)
219 RF of 229 FR and 237 RF] of DNA motif sequences, which included CTCF, cohesin
220 (RAD21 and SMC3), ZNF143 and YY1 in two replications (B1 and B2), a significantly
221 higher ratio of EPIs overlapped with HiChIP chromatin interactions in EPA (i) than the
222 other types of EPA (ii) and (iii) (Supplemental material). When comparing EPIs
223 predicted based on only EPA (i) and (iii) with the chromatin interactions, for total 366
224 biased orientations [218 (95%) FR and 227 (96%) RF of 229 FR and 237 RF] of DNA
225 motif sequences, a significantly higher ratio of EPIs overlapped with the chromatin
226 interactions in EPA (i) than EPA (iii) (Supplemental material).

227 In situ Hi-C data in HMEC, which are available in 4D nucleome data portal, were
228 compared with putative EPIs. The number of unique in situ Hi-C cis chromatin
229 interactions was 121,873,642 at 3 kb resolution. For total 222 biased orientations [155
230 (50%) FR and 108 (40%) RF of 310 FR and 269 RF] of DNA motif sequences, which

231 included CTCF, cohesin (RAD21 and SMC3), ZNF143 and YY1, a significantly higher
232 ratio of EPIs overlapped with in situ Hi-C chromatin interactions (≥1 count for each
233 interaction, i.e. all interactions) in EPA (i) than the other types of EPA (ii) and (iii)
234 (Supplemental material). When comparing EPIs predicted based on only EPA (i) and
235 (iii) with the chromatin interactions, for total 406 biased orientations [268 (86%) FR
236 and 230 (86%) RF of 310 FR and 269 RF] of DNA motif sequences, a significantly
237 higher ratio of EPIs overlapped with the chromatin interactions in EPA (i) than EPA (iii)
238 (Supplemental material). There were six replications of in situ Hi-C experimental data
239 of HMEC, but other replications contained much smaller number of chromatin
240 interactions. The HiChIP chromatin interaction data in T cells were expected to be
241 enriched with enhancer-promoter interactions, since they were produced with H3K27ac
242 antibody to capture chromatin interactions. In situ Hi-C data consist of all types of
243 chromatin interactions and thus, contain a smaller number of enhancer-promoter
244 interactions than HiChIP data. Chromatin interactions with a small number of counts
245 may be artifacts occurred by ligation errors during experiments (Lieberman-Aiden et al.
246 2009; Yardimci et al. 2019). Therefore, other replications of in situ Hi-C data with a
247 smaller number of chromatin interactions will not be available for this analysis.

248 Promoter capture Hi-C data of NPC was downloaded and analyzed in the same
249 procudure as T cell and HMEC (Jung et al. 2019). The number of unique promoter
250 capture Hi-C cis chromatin interactions was 9,436,689 at 5 kb resolution. For total 109
251 biased orientations [61 (28%) FR and 60 (25%) RF of 205 FR and 241 RF] of DNA
252 motif sequences, which included CTCF, cohesin (RAD21 and SMC3), ZNF143 and

253 YY1, a significantly higher ratio of EPIs overlapped with promoter capture Hi-C
254 chromatin interactions (≥1 count for each interaction, i.e. all interactions) in EPA (i)
255 than the other types of EPA (ii) and (iii) (Supplemental material). When comparing EPIs
256 predicted based on only EPA (i) and (iii) with the chromatin interactions, for total 186
257 biased orientations [99 (48%) FR and 103 (43%) RF of 205 FR and 241 RF] of DNA
258 motif sequences, a significantly higher ratio of EPIs overlapped with the chromatin
259 interactions in EPA (i) than EPA (iii) (Supplemental material).

260 All three types of chromatin interaction data (HiChIP, in situ Hi-C and promoter
261 capture Hi-C) indicated that EPIs predicted based on EPA (i) that was shortened at DNA
262 motif sites of known TFs involved in chromatin interactions (CTCF, RAD21, SMC3,
263 ZNF143 and YY1), overlapped with more chromatin interactions than the other EPA (ii)
264 and (iii) in six cell types (T cells, Th17, Treg, GM12878, HMEC and NPC). In
265 monocyte, Hi-C data was available, but it was not analyzed, due to the low resolution of
266 chromatin interaction data (50 kb).

267 The biased orientations of DNA motif sites of known TFs involved in chromatin
268 interactions such as CTCF, RAD21, SMC3, YY1 and ZNF143 may be overlapped with
269 the biased orientations of DNA motif sites of other TFs, and thus, they showed a
270 significantly higher ratio of EPIs overlapped with chromatin interactions in EPA (i) than
271 the other types of EPA (ii) and (iii). However, among 273 FR and 211 RF orientations of
272 DNA motifs of TFs not including the known TFs in T cells, the DNA motif sites of only
273 15 (6%) FR and 9 (4%) RF orientations of DNA motifs of TFs overlapped with ≥ 60%
274 of DNA motif sites of biased orientations of DNA motifs of either of the known TFs at 5

275 kb resolution.

276 Moreover, to investigate the enhancer activity of EPIs, the distribution of
277 expression level of putative target genes of EPIs was compared between EPIs
278 overlapped with HiChIP chromatin interactions and EPIs not overlapped with them.
279 Though the target genes of EPIs were selected from top 4,000 transcripts (genes) in
280 terms of the expression level of all transcripts (genes) excluding transcripts not
281 expressed in T, Th17, Treg and GM12878 cells separately, target genes of EPIs
282 overlapped with chromatin interactions indicated a significantly higher expression level
283 than EPIs not overlapped with them, suggesting that EPIs overlapped with chromatin
284 interactions activated the expression of target genes in the four cell types. For almost all
285 (99% - 100%) FR and RF orientations of DNA motifs, a significantly higher expression
286 level of putative target genes of EPIs overlapped with chromatin interactions than EPIs
287 not overlapped in the four cell types. When a biased orientation of DNA motif showed a
288 significantly higher expression level of putative target genes of EPIs overlapped with
289 chromatin interactions than EPIs not overlapped, '1' was marked with in the tables of
290 comparison between EPIs and HiChIP chromatin interactions in Supplemental material.
291 DNA motifs showing a significantly lower expression level or not showing a significant
292 difference of expression level were not observed in this analysis. HiChIP data were
293 produced using H3K27ac antibody, so chromatin interactions acting as repressor would
294 not be identified. However, for in situ Hi-C and promoter capture Hi-C data in HMEC
295 and NPC, the significant difference of expression level of putative target genes of EPIs
296 was observed in a small percentage (less than 1%) of biased orientations of DNA

297 motifs.

298

299 **Correlation of expression level of gene pairs separated by DNA motif sites of a TF**

300 To ask whether the biased orientations of DNA motif sites affect gene expression,
301 I compared the expression level of protein-coding genes the most closely located to
302 upstream and downstream of biased orientations of DNA motif sites in the human
303 genome. The expression levels of closely located genes including divergent gene pairs
304 tend to be correlated among tissues (Purmann et al. 2007; Xie et al. 2007). When a
305 biased orientation of DNA motif sites serve as insulator (e.g. CTCF), the correlation of
306 gene expression level would be reduced. Among 96 biased (64 FR and 52 RF)
307 orientations of DNA motifs of TFs found in common in monocytes, T cells, HMEC and
308 NPC, TFs with ≥50 genomic locations of the DNA motif sites were selected, after the
309 elimination of ubiquitously expressed genes among 53 tissues and DNA motif sites near
310 the genes with coefficient of variance (CV) <90. After this filtering, 43 (72%) FR and
311 40 (80%) RF of 60 FR and 50 RF showed significantly lower correlations of expression
312 levels of gene pairs separated by the DNA motif sites of a TF than the correlations of all
313 pairs of neighbor genes with intergene distance <1 megabase (Mb) (Mann-Whitney test,
314 p-value < 0.05) (Table 3). The FR and RF orientations of TFs included known TFs
315 involved in chromatin interactions such as CTCF, RAD21, SMC3, YY1 and ZNF143.
316 Top 20 of the FR and RF orientations of DNA motifs were selected in ascending order
317 of the median correlation coefficient of expression levels of gene pairs separated by the
318 DNA motif sites of a TF. The 20 TFs included known TFs involved in chromatin

319 interactions such as CTCF, RAD21 and SMC3 (Fig. 4) (Mann-Whitney test, *p*-value <
320 0.01). Instead of using all DNA motif sites of a TF, when DNA motif sites of a TF were
321 limited to sites examined for biased orientations of DNA motifs in an EPA, 33 (60%)
322 FR and 36 (77%) RF of 55 FR and 47 RF showed significantly lower correlations of
323 expression levels of gene pairs separated by the DNA motif sites (Supplemental
324 material). With intergene distance <20 kb, 21 (34%) FR and 8 (15%) RF of 62 FR and
325 52 RF showed significantly lower correlations of expression levels of gene pairs
326 separated by the DNA motif sites of a TF than the correlations of all pairs of neighbor
327 genes (Supplemental material).

328 A large number of DNA motif sites of a TF tend to show significantly lower
329 correlations of gene expression (Median numbers of DNA motif sites showing
330 significantly lower correlations were 656 and 479 for FR and RF respectively, and
331 median numbers of DNA motif sites not showing lower correlations significantly were
332 122 and 115 for FR and RF respectively. Mann-Whitney test *p*-value = 0 and < 10^{-10} for
333 FR and RF respectively). This suggests that if the criteria to examine the correlations of
334 expression levels of gene pairs separated by DNA motif sites are more stringent, and
335 thus the number of DNA motif sites is reduced, it would be more difficult to identify
336 using a statistical test the difference of correlations of expression levels of gene pairs
337 separated by the reduced DNA motif sites of TFs, particularly for TFs with a small
338 number of DNA motif sites.

339 Among 91 biased orientations of DNA motifs of TFs found in common in the
340 four cell types, after removing five known TFs involved in chromatin interactions such

341 as CTCF, RAD21, SMC3, YY1 and ZNF143, DNA motif sites of 88 TFs were located
342 at ≥1 genomic regions between gene pairs not including DNA motif sites of the known
343 TFs, and at ≥1 genomic regions between a low correlation (< 0.13) of expression level
344 of gene pairs (when ubiquitously expressed genes among 53 tissues were eliminated
345 with CV <90. The median correlation coefficient of expression level of all pairs of
346 nearby genes is 0.17, Table 3). DNA motif sites of 52 TFs were placed at ≥10 genomic
347 regions.
348
349 **Co-location of biased orientations of DNA motif sites of TFs**
350 To examine the association of biased orientations of DNA binding motif
351 sequences of TFs, co-location of the DNA binding motif sequences within 200bp to
352 each other, which is close to the length of core DNA around octamer of core histone
353 (146bp), that is, the length of the minimum open chromatin region, was analyzed in
354 monocytes, T cells, HMEC and NPC. The same pairs of DNA binding motif sequences
355 in upstream and downstream of genes in EPAs were enumerated, and the pairs of DNA
356 binding motif sequences found in ≥100 genomic regions were listed (Table 4;
357 Supplemental material). Majority of pairs of DNA motif sites overlapped with more
358 than 1 base, but the same tendency was found in the analysis of DNA motif sites of all
359 TFs (Supplemental material). CTCF was partially overlapped with cohesin RAD21 and
360 SMC3 (Table 4). Top 30 pairs of FR and RF orientations of DNA motifs overlapped or
361 co-localized were shown (Table 4). Total numbers of unique pairs of DNA motif sites of
362 TFs overlapped or co-localized were 404 (FR) and 662 (RF) in monocytes, consisting of

363 177 (39% of all FR) and 218 (43% of all RF) unique DNA motifs. Only ten overlapping
364 or co-location of DNA motifs of TFs were identified in the four cell types in common,
365 including pairs of CTCF, RAD21, SMC3 and YY1. This implies that most of
366 overlapping and co-location of DNA motifs of TFs serve in cell-type-specific manner
367 (Supplemental material). Pairs of biased orientations of DNA binding motifs of TFs
368 tend to overlap, and relatively a small number of motifs are co-localized in upstream
369 and downstream of genes. Overlapping DNA motifs act as DNA binding sites of several
370 TFs simultaneously or competitively (Ackerman et al. 1991; Yoon and Chikaraishi
371 1992; Ansari and Peterson-Kaufman 2011; Slattery et al. 2011; Chatterjee et al. 2012;
372 He et al. 2015; Kin et al. 2016; Merabet and Mann 2016). CTCF and cohesin function
373 coordinately with another TF and a protein such as Klf4 and Brd2 (Wei et al. 2013; Hsu
374 et al. 2017). Klf4 recruits cohesin to the Oct4 enhancer region. BRD2 supports
375 boundary (insulator) activity of CTCF. The analysis of 457 ChIP-seq data sets on 119
376 human TFs showed that secondary motifs were detected in addition to the canonical
377 motifs of the TFs, indicating tethered binding and co-binding between multiple TFs
378 (Wang et al. 2012a). The authors observed significant position and orientation
379 preferences between many co-binding TFs. Overlapping DNA motif sites of TFs found
380 in this study may not be artifact, but biologically functional. Though repeat sequences in
381 human genome were masked, more than a hundred of pairs of DNA motif sites
382 overlapped at hundreds or thousands upstream and downstream regions of genes.
383

384 **Discussion**

385 The approach in this study is an initial comprehensive method to find DNA motif
386 sequences of transcription factors (TFs) associated with chromatin interaction and
387 insulator function. DNA motif sequences were searched from open chromatin regions of
388 monocytes, T cells, HMEC and NPC. Total 96 biased [64 forward-reverse (FR) and 52
389 reverse-forward (RF)] orientations of DNA motif sequences of TFs were found in the
390 four cell types in common, whereas non-orientation (i.e. without considering
391 orientation) of DNA motif sequences of TFs were not found to affect the expression
392 level of putative transcriptional target genes, suggesting that an enhancer-promoter
393 association (EPA) shortened at the FR or RF orientation of DNA motif sites of a TF
394 includes more accurate prediction of enhancer-promoter interactions (EPIs), which were
395 supported by the comparisons with chromatin interaction and gene expression data.
396 To predict DNA motif sites of TFs, I tried several tools and methods, and then
397 used protein interaction quantitation (PIQ) tool (Sherwood et al. 2014). PIQ predicts
398 DNA motif sites of TFs by reducing noises of DNase-seq data, and the comparison of
399 the prediction with ChIP-seq data has revealed that PIQ shows a better performance
400 than other tools and digital genome footprinting (DNase-DGF). The prediction of DNA
401 motif sites of TFs using PIQ in this study increased the number of biased orientations of
402 DNA motif sequences of TFs, reducing the number of non-orientation of DNA motif
403 sequences of TFs. At first, the number of predicted DNA motif sites of TFs was
404 expected to increase, relative to using consensus DNA sequences of TFs, which seemed
405 to be stringent to find all DNA motif sites of a TF in the genome. However, the number
406 of DNA motif sites was almost the same or slightly decreased, compared with the

407 analysis of consensus DNA sequences, suggesting that PIQ increases true positive
408 predictions of DNA motif sites, reducing false positive predictions.

409 When forming a homodimer or heterodimer with another TF, TFs may bind to
410 genome DNA with a specific orientation of their DNA binding sequences (Fig. 5). The
411 approach in this study would be able to identify TFs forming heterodimer. If the DNA
412 motif site of only the mate to a pair of TFs was found in an EPA, the EPA was shortened
413 at one side of the DNA motif site, and transcriptional target genes were predicted based
414 on the EPA shortened at the side. In this analysis, the mate to both heterodimer and
415 homodimer of TFs can be tested to examine the effect on the expression level of
416 transcriptional target genes predicted based on the EPA shortened at one side. Biased
417 orientations of DNA motif sequences may also be found in forward-forward or
418 reverse-reverse orientation.

419 TFs that are multi-functional transcriptional regulator such as YY1 may not
420 indicate a strong biased orientation of their DNA motif sites. Though some proportion
421 of DNA motif sites of a TF involved in chromatin interaction and insulator function lie
422 in biased orientation in the genome, the other DNA motif sites of the TF may not form a
423 dimer with another TF, and not be present in a specific orientation in the genome. Thus,
424 overall proportion of biased orientations of DNA motif sites of a TF may be reduced, so
425 that a statistical test cannot detect it.

426 The approach in this study was tested to search for repeat sequences serving as
427 insulator sites and affecting the expression level of putative transcriptional target genes
428 of TFs. A small number of repeat sequences were identified and included MIR, which

429 acts as insulators (Wang et al. 2015).

430 CTCF and cohesin-binding sites are frequently mutated in cancer (Katainen et al.
431 2015). Some biased orientations of DNA motif sequences would be involved in
432 chromatin interactions and might be associated with diseases including cancer.

433 The analyses taken here suggest that biased orientations of DNA motifs of
434 discovered insulator TFs affect enhancer-promoter interactions and the expression level
435 of putative transcriptional target genes of general TFs bound in enhancers and
436 promoters through insulator function. This gives insight into the nature of insulators and
437 contributes to the researches of functions and molecular mechanisms of chromatin
438 interactions, TFs, transcriptional regulation and transcriptional cascades.

439

440 ## Methods

441 **Search for biased orientations of DNA motif sequences**

442 To identify transcription factor binding sites (TFBSs) from open and closed
443 chromatin regions, TRANSFAC (2019.2), JASPAR (2018), UniPROBE (2018),
444 high-throughput SELEX, transcription factor binding sequences of ENCODE ChIP-seq
445 data, and HOCOMOCO version 9 and 11 were used to predict insulator sites
446 (Wingender et al. 1996; Newburger and Bulyk 2009; Portales-Casamar et al. 2010; Xie
447 et al. 2010; Zhao and Stormo 2011; Jolma et al. 2013; Kheradpour and Kellis 2014;
448 Kulakovskiy et al. 2018). TRANSFAC (2019.2) was used to analyze enhancer-promoter
449 interactions, because these data were sufficient to identify biased orientations of DNA
450 motif sequences of insulator TFs with less computational time, reducing the number of

451 non-orientation of DNA motif sequences of TFs. To reduce false positive prediction of
452 DNA motif sites of TFs in open chromatin regions, DNA motif search was performed
453 by protein interaction quantitation (PIQ) tool with 12,249 position frequency matrices
454 converted from DNA motifs of vertebrate TFs in the above databases and DNase-seq
455 data from GEO and ENCODE database (GSM1024791 $CD14^+$ monocytes; GSM665812
456 $CD4^+$ T cell; GSM736634 Human mammary epithelial cell, HMEC; GSM878615
457 Neural progenitor cell, NPC; ENCFF263GMV, ENCFF886XEV Th17; GSM1024741
458 Treg; GSM736620 GM12878) (Sherwood et al. 2014). To find open chromatin regions
459 associated with enhancer (and promoter) activity, narrow peaks of ChIP-seq
460 experimental data of H3K27ac were predicted using macs2 callpeak (GEO:
461 GSM773004) (Zhang et al. 2008). To predict DNA motif sites of TFs from closed
462 chromatin regions, another method was employed. Position weight matrices of
463 vertebrate transcription factor binding sequences were converted into DNA consensus
464 sequences, which consist of alphabet of 15 characters (the four bases A, C, G, T, the six
465 two-fold degenerate IUPAC codes R=[AG], Y=[CT], K=[GT], M=[AC], S=[GC],
466 W=[AT], the four three-fold degenerate IUPAC codes B=[CGT], D=[AGT], H=[ACT],
467 V=[ACG], and the four-fold degenerate character N=[ATGC]) using convert matrix in
468 RSAT website (van Helden 2003). Transcription factor binding sequences were
469 searched from narrow peaks of DNase-seq data in repeat-masked hg19 genome
470 sequences using Match tool in TRANSFAC with similarity score cutoff of 1 after
471 transforming the DNA consensus sequences of TFs into position frequency matrixes for
472 Match search (Kel et al. 2003). Repeat-masked hg19 genome sequences were

473 downloaded from UCSC genome browser (http://genome.ucsc.edu/,
474 http://hgdownload.soe.ucsc.edu/goldenPath/hg19/bigZips/hg19.fa.masked.gz). TFs
475 corresponding to transcription factor binding sequences were searched computationally
476 and manually by comparing their names and gene symbols of HGNC (HUGO Gene
477 Nomenclature Committee) -approved gene nomenclature and 31,848 UCSC known
478 canonical transcripts
479 (http://hgdownload.soe.ucsc.edu/goldenPath/hg19/database/knownCanonical.txt.gz),
480 because transcription factor binding sequences were not linked to transcript IDs such as
481 UCSC, RefSeq and Ensembl transcripts.

482 Target genes of a TF were assigned when its TFBS was found in DNase-seq
483 narrow peaks in promoter or extended regions of enhancer-promoter association of
484 genes (EPA). Promoter and extended regions were defined as follows: promoter regions
485 were those that were within distance of ±5 kb from transcriptional start sites (TSS).
486 Promoter and extended regions were defined as per the following association rule,
487 which is the same as that defined in Figure 3A of a previous study (McLean et al. 2010):
488 the single nearest gene association rule, which extends the regulatory domain to the
489 midpoint between the TSS of the gene and that of the nearest gene upstream and
490 downstream without the limitation of extension length. The limitation of extension
491 length was ＜1 Mb in this study. Extended regions for an EPA were shortened at the
492 DNA motif sites of a putative insulator TF that were the closest to a TSS, and
493 transcriptional target genes were predicted based on the shortened EPA and DNA motif
494 sites of a general TF in open chromatin regions. Promoter and extended regions of an

495 EPA were shortened at the forward–reverse (FR) orientation of DNA binding sites of a
496 putative insulator TF. When forward or reverse orientation of DNA binding sites were
497 continuously located in the genome several times, the most internal (i.e. closest to a
498 TSS) forward–reverse orientation of DNA binding sites were selected. The genomic
499 positions of genes were identified using 'knownGene.txt.gz' file in UCSC
500 bioinformatics sites (Karolchik et al. 2014). The file 'knownCanonical.txt.gz' was also
501 utilized to select representative transcripts among various alternate forms for assigning
502 promoter and extended regions of an EPA. From the list of transcription factor binding
503 sequences and transcriptional target genes, redundant transcription factor binding
504 sequences were removed by comparing the putative target genes of a transcription
505 factor binding sequence and its corresponding TF; if identical, one of the transcription
506 factor binding sequences was chosen. When the number of transcriptional target genes
507 predicted based on a transcription factor binding sequence was less than five, the
508 transcription factor binding sequence was omitted.

509 For gene expression data, RNA-seq reads mapped onto the human hg19 genome
510 sequence were obtained from UCSF-UBC human reference epigenome mapping project
511 RNA-seq reads with poly-A of naive $CD4^+$ T cells (GEO: GSM669617). For monocytes,
512 Blueprint RNA-seq FPKM data
513 ('C0010KB1.transcript_quantification.rsem_grape2_crg.GRCh38.20150622.results')
514 were downloaded from Blueprint DCC portal
515 (http://dcc.blueprint-epigenome.eu/#/files). RNA-seq reads with poly-A of human
516 mammary epithelial cells (HMEC) in Encyclopedia of DNA Elements at UCSC

517 (http://genome.ucsc.edu/encode/,

518 'wgEncodeCshlLongRnaSeqHmecCellPapAlnRep1.bam' file), H1 derived neural

519 progenitor cell (NPC) (GEO: GSM915326, ENCODE: ENCFF529SIO), Th17

520 (GSM2859479, NCBI SRA: SRR6298326), Treg (GSM2859476, SRR6298323) and

521 GM12878 (GSE78551, ENCFF297QCE) were analyzed. RNA-seq reads were aligned

522 in repeat-masked hg19 genome sequences using BWA with default parameters (Li and

523 Durbin 2009). FPKMs of the RNA-seq data were calculated by RSeQC (Wang et al.

524 2012b). Based on log2-transformed FPKM, UCSC transcripts were arranged in

525 descending order of expression level, and top 4,000 transcripts were selected in each

526 cell type.

527 The expression level of transcriptional target genes predicted based on EPAs

528 shortened at the DNA motif sites of a TF was compared with the expression level of

529 transcriptional target genes predicted based on closed chromatin regions in promoters.

530 For each DNA motif sequence shortening EPAs, transcriptional target genes were

531 predicted based on DNA binding motif sequences of vertebrate TFs in TRANSFAC

532 database, and the ratio of expression level of putative transcriptional target genes of

533 each TF was calculated between an EPA and closed chromatin regions in promoters.

534 The distribution of the ratios of all TFs was compared among forward-reverse (FR),

535 reverse-forward (RF) and non-orientation (i.e. without considering orientation) of a

536 DNA motif sequence shortening an EPA using Mann-Whitney test, two-sided (p-value <

537 10^{-7}). Other parameters for the analysis were set as follows: the number of

538 transcriptional target genes of a TF was $\geq$50, the number of general TFs (not insulator

539 TFs) to predict transcriptional target genes was ≥50, and the number of DNA motif
540 sites of a TF (insulator TF) shortening an EPA was ≥100.
541
542 **Comparison with chromatin interaction data**
543 For comparison of EPIs with chromatin interactions (HiChIP) in $CD4^+$ T, Th17,
544 Treg and GM12878 cells,
545 'GSM2705049_Naive_HiChIP_H3K27ac_B2T1_allValidPairs.txt',
546 'GSM2705050_Naive_HiChIP_H3K27ac_B2T2_allValidPairs.txt',
547 'GSM2705051_Naive_HiChIP_H3K27ac_B3T1_allValidPairs.txt',
548 'GSM2705054_Th17_HiChIP_H3K27ac_B1T2_allValidPairs.txt',
549 'GSM2705055_Th17_HiChIP_H3K27ac_B2T1_allValidPairs.txt',
550 'GSM2705056_Th17_HiChIP_H3K27ac_B3T1_allValidPairs.txt',
551 'GSM2705059_Treg_HiChIP_H3K27ac_B3T1_allValidPairs.txt',
552 'GSM2705041_GM_HiChIP_H3K27ac_B1_allValidPairs.txt',
553 'GSM2705042_GM_HiChIP_H3K27ac_B2_allValidPairs.txt' files were downloaded
554 from Gene Expression Omnibus (GEO) database. The resolutions of chromatin
555 interactions and EPIs were adjusted to 5 kb before their comparison. Chromatin
556 interactions with ≥6,000 and ≥1,000 counts for each interaction were analyzed in the
557 comparison in $CD4^+$ T cells. According to the unique numbers of chromatin interactions
558 in replications in Th17, Treg and GM12878 cells, chromatin interactions with ≥1,000
559 (B1T2 in Th17), ≥2,000 (B2T1 and B3T1 in Th17), ≥6,000 (B3T1 in Treg), ≥4,000
560 (B1 and B2 in GM12878) counts for each interaction were analyzed in the comparison.

561 Enhancer-promoter interactions (EPIs) were predicted based on three types of
562 EPAs in monocytes: (i) EPA shortened at the FR or RF orientation of DNA motif sites
563 of a TF, (ii) EPA shortened at the non-orientation (i.e. without considering orientation)
564 of DNA motif sites of a TF, and (iii) EPA without being shortened by a DNA motif site.
565 EPIs predicted based on the three types of EPAs in common were removed. EPIs
566 predicted based on EPA (i) were removed from EPIs predicted based on EPA (ii). EPIs
567 predicted based on EPA (i) and (ii) were removed from EPIs predicted based on EPA
568 (iii). The resolution of HiChIP chromatin interaction data was 1-5 kb, so EPIs were
569 adjusted to 5 kb before their comparison. The number and ratio of EPIs overlapped with
570 chromatin interactions were compared two times between EPI (i) and (iii), and EPI (i)
571 and (ii) (binomial distribution, p-value < 0.025 for each test, two-sided, 95% confidence
572 interval).

573 For comparison of EPIs with chromatin interactions (in situ Hi-C) in HMEC, the
574 genomic positions of chromatin interactions in 'HMEC_4DNFI97O9SAZ.pairs.gz' file
575 in 4D nucleome data portal (http://data.4dnucleome.org) were converted into hg19
576 version of human genome using liftOver tool
577 (http://hgdownload.soe.ucsc.edu/downloads.html#liftover). The resolutions of
578 chromatin interaction data and EPIs were adjusted to 3 kb before their comparison. All
579 chromatin interactions were used in the comparison. For comparison of EPIs with
580 chromatin interactions (promoter capture Hi-C) in NPC, the resolutions of chromatin
581 interaction data in 'GSE86189_npc.po.all.txt.bz2' file (GEO: GSE86189) and EPIs were
582 adjusted to 5 kb before their comparison. All chromatin interactions were used in the

583 comparison.

584 Putative target genes for the comparison of EPIs and chromatin interactions were
585 selected from top 4,000 transcripts in term of the expression level. The expression level
586 of putative target genes of EPIs overlapped with chromatin interactions was compared
587 with EPIs not overlapped with them. When the same transcriptional target gene of a TF
588 in an enhancer was predicted based on both an EPI overlapped with a chromatin
589 interaction and an EPI not overlapped with, the target gene was eliminated. The
590 distribution of expression level of putative target genes was compared using
591 Mann-Whitney test, two-sided (p-value < 0.05).

592

593 **Correlation of expression level of gene pairs separated by DNA motif sites of a TF**

594 To examine the correlation of expression level of genes pairs separated by DNA
595 motif sites of a TF, gene expression data among 53 tissues were obtained from
596 'GTEx_Analysis_2016-01-15_v7_RNASeQCv1.1.8_gene_median_tpm.gct.gz' file in
597 GTEx database (https://gtexportal.org/home/). The correlation of log2-transformed gene
598 expression level was analyzed based on protein-coding transcripts of RefSeq (RefSeq
599 ID with 'NM_'). The same genomic location of RefSeq transcripts were removed. DNA
600 motif sites overlapped with RefSeq transcripts were eliminated. Genes closest to a DNA
601 motif sites and another gene were analyzed using BEDOPS closest-features (Neph et al.
602 2012). Mann-Whitney test was performed using R.

603

604 **Acknowledgements**

605 The supercomputing resource was provided by Human Genome Center of the Institute
606 of Medical Science at the University of Tokyo. Computations were partially performed
607 on the NIG supercomputer at ROIS National Institute of Genetics. Publication charges
608 for this article were funded by JSPS KAKENHI Grant Number 16K00387. This
609 research was partially supported by the Platform Project for Supporting in Drug
610 Discovery and Life Science Research（Platform for Dynamic Approaches to Living
611 System）from Japan Agency for Medical Research and Development (AMED). This
612 research was partially supported by Development of Fundamental Technologies for
613 Diagnosis and Therapy Based upon Epigenome Analysis from Japan Agency for
614 Medical Research and Development (AMED). This work was partially supported by
615 JST CREST Grant Number JPMJCR15G1, Japan.
616

617 **Figures**

618 Web links to original figures.

619 Figure 1. (A) Figure 1. Enhancers and their features. (Shlyueva et al. 2014)

620 https://static-content.springer.com/esm/art%3A10.1038%2Fnrg3682/MediaObjects/415

621 76_2014_BFnrg3682_MOESM18_ESM.ppt

622 Graphical Abstract (de Wit et al. 2015)

623 https://marlin-prod.literatumonline.com/cms/attachment/7d219941-8398-4373-9ac9-8bf

624 92c5eba1d/fx1.jpg

625

626 (B) Supplementary Figure 2. Computationally-defined regulatory domain (McLean et al.

627 2010)

628 https://static-content.springer.com/esm/art%3A10.1038%2Fnbt.1630/MediaObjects/415

629 87_2010_BFnbt1630_MOESM11_ESM.pdf

630 Figure 4. The Role of CBS Location and Orientation in CTCF-Mediated Genome-wide

631 DNA Looping (Guo et al. 2015)

632 https://marlin-prod.literatumonline.com/cms/attachment/297a06ad-7568-483e-9904-9ae

633 2af081251/gr4.jpg

634

635 **Figure 1.** Chromatin interaction and enhancer-promoter association. (A) Forward–

636 reverse orientation of CTCF-binding sites are frequently found in chromatin interaction

637 anchors. CTCF can block the interaction between enhancers and promoters limiting the

638 activity of enhancers to certain functional domains (Rao et al. 2014; Shlyueva et al.

639 2014; de Wit et al. 2015; Guo et al. 2015). (B) Computationally-defined regulatory
640 domains for enhancer-promoter association (McLean et al. 2010). The *single nearest*
641 *gene* association rule extends the regulatory domain to the midpoint between this gene's
642 TSS and the nearest gene's TSS both upstream and downstream. The enhancer-promoter
643 association was shortened at the forward-reverse orientation of DNA binding motif sites
644 of a TF in this study (e.g. CTCF in the figure).
645

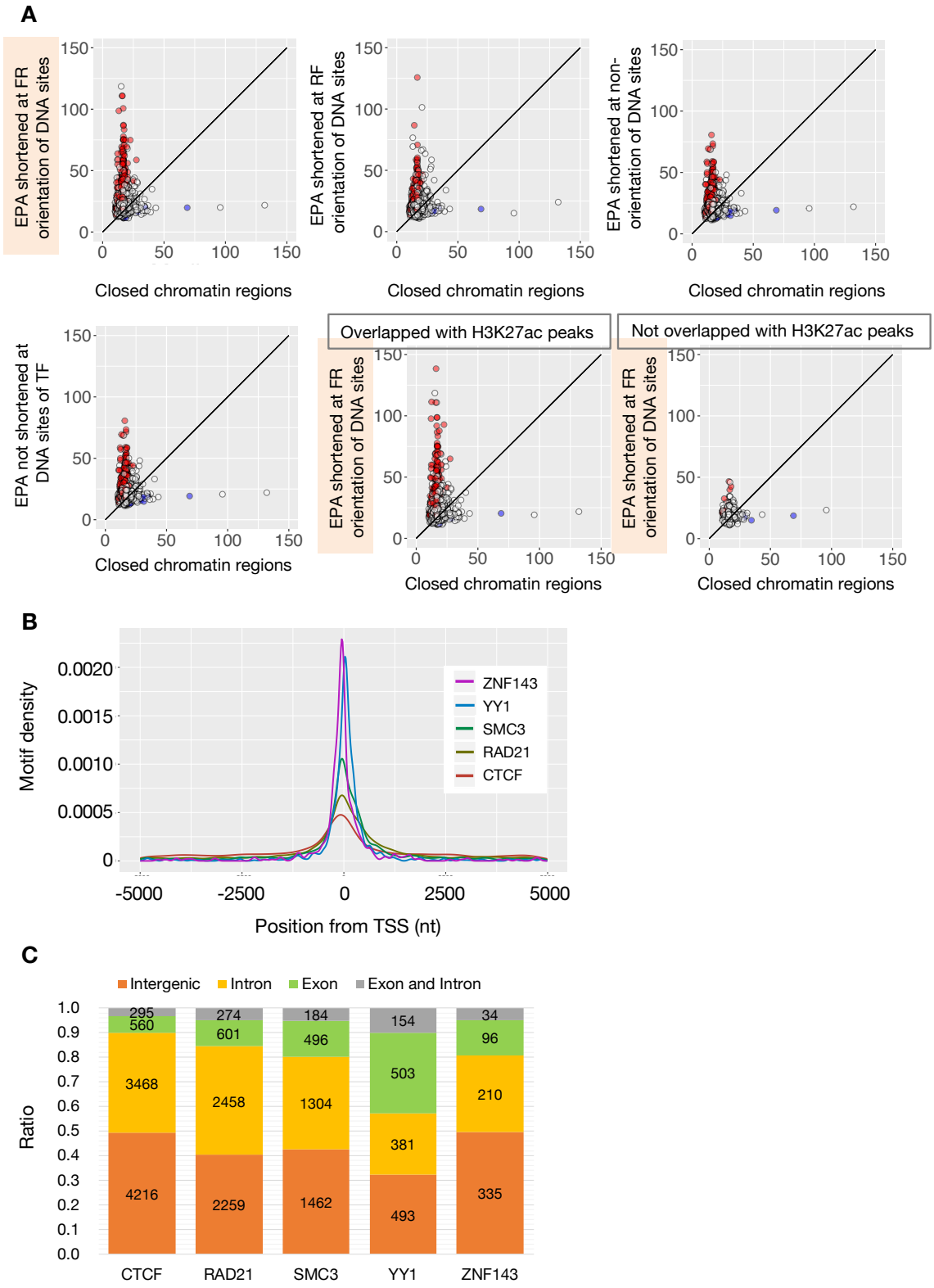

Figure 2. Identification of DNA motif sites of TFs from open chromatin regions and properties of DNA motif sites of TFs. (A) Comparison of expression level of putative

649 transcriptional target genes. Each dot represents the median expression level (FPKM) of
650 target genes predicted based on DNA motif sites of a transcription factor in closed
651 chromatin regions in promoters (X-axis) and an enhancer-promoter association (EPA)
652 shortened at the forward-reverse orientation of DNA motif sites of CTCF (Y-axis) in T
653 cell (upper left graph). The distribution of expression level was changed according to
654 four criteria of EPAs (four graphs) (Osato 2018). Red dots indicate the median
655 expression level of target genes was significantly higher in an EPA than closed
656 chromatin regions, and blue dots indicate the median expression level of target genes
657 was significantly lower in an EPA than closed chromatin regions (Mann-Whitney test).
658 The expression level of target genes predicted based on an EPA tend to be higher than
659 closed chromatin regions, implying that TFs serve as activators of target genes. DNA
660 motif sites of TFs overlapped with H3K27ac ChIP-seq peaks were associated with a
661 significant difference of expression level of target genes, and DNA motif sites not
662 overlapped with H3K27ac peaks were not associated with the difference (lower right
663 two graphs). This suggests that the significant difference of expression level is
664 associated with enhancer (and promoter) signals of H3K27ac. (B) Distribution of DNA
665 motif sites of TFs near TSS. ZNF143 and YY1 tend to be located near TSS, and CTCF
666 tend to be observed more in distant regions than around TSS in monocyte. (C)
667 Distribution of DNA motif sites of TFs in the human genome in monocytes. Most of
668 DNA motif sites were found in intergenic and intron regions. YY1 is known to be at
669 TSS in the edge of exons of genes, and is involved in transcriptional activation,
670 repression and initiation.

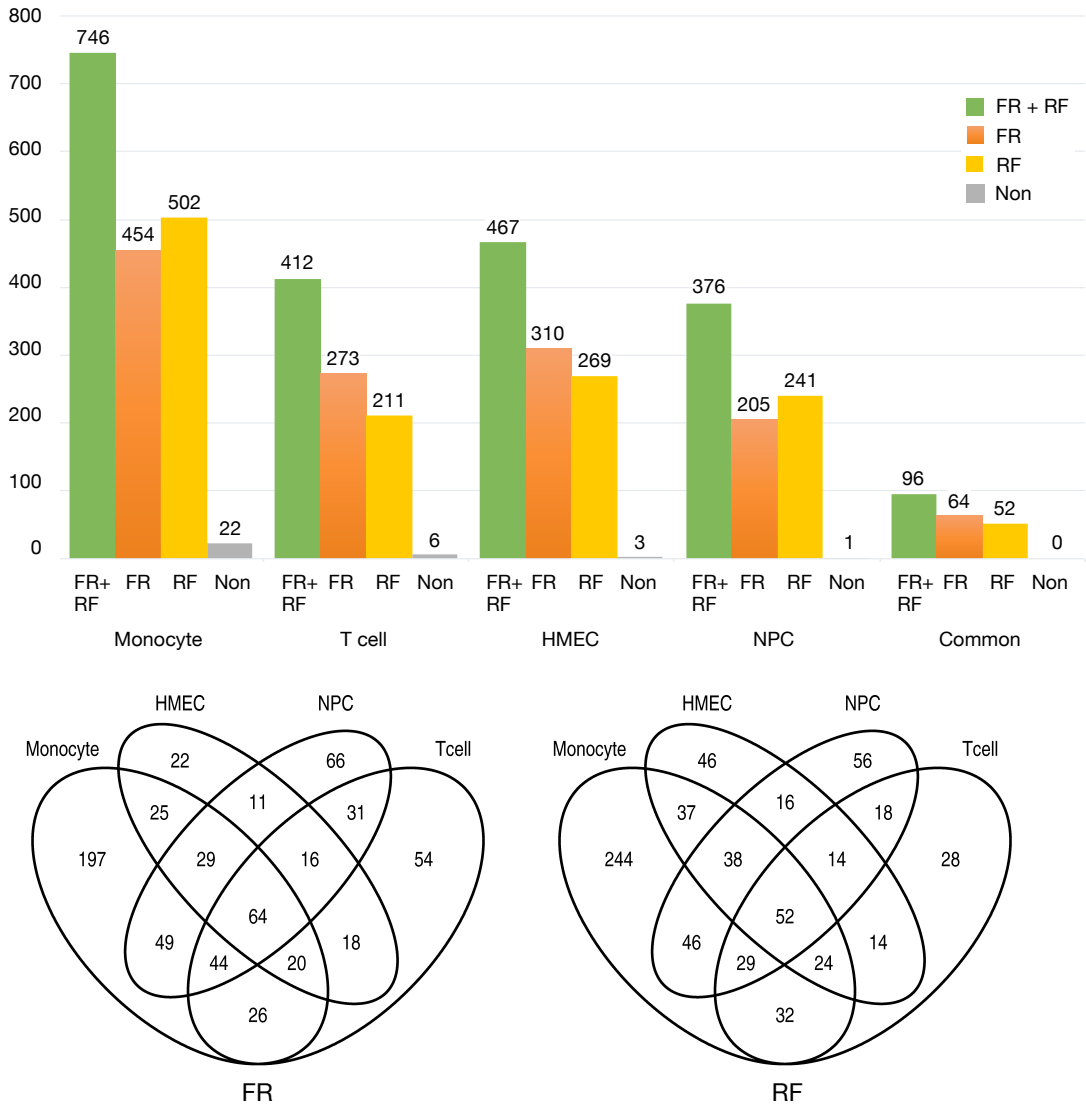

Figure 3. Biased orientations of DNA motif sequences of TFs affect the transcription of genes by the putative insulator function of the DNA motif sites. Total 96 (64 FR and 52 RF) of biased orientations of DNA binding motif sequences of TFs affected significantly the expression level of putative transcriptional target genes in monocytes, T cells, HMEC and NPC in common, whereas non-orientation (i.e. without considering

678 orientation) of DNA binding motif sequence of a TF did not affect the expression level

679 significantly.

680

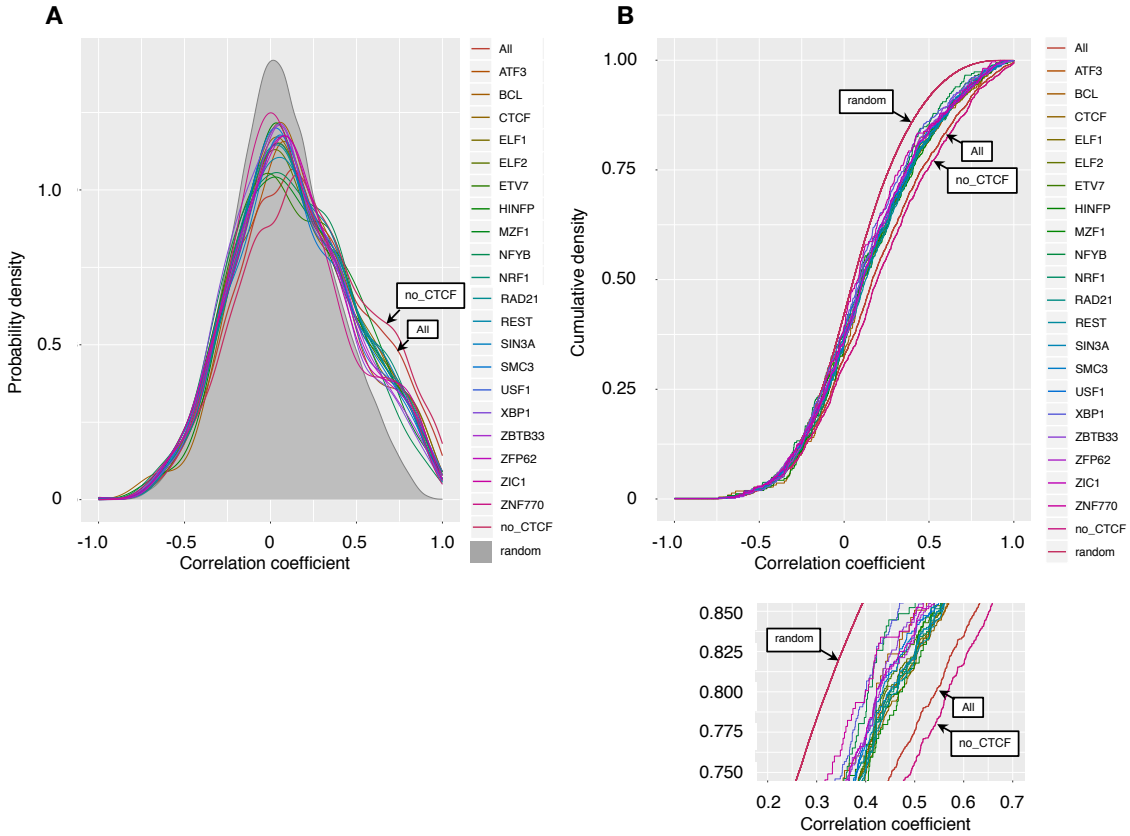

681

682 **Figure 4.** Genes separated by predicted DNA binding sites of biased orientations of

683 DNA motifs of TFs are less correlated in gene expression. Top 20 TFs are selected

684 according to ascending order of median correlation coefficient. Correlation coefficient

685 between neighboring gene pairs is shown in terms of probability density (A) and

686 cumulative distribution (B). Brown line (All), correlation between all neighboring

687 genes; gray shading in (A) and red line (random) in (B), correlation between randomly

688 chosen gene pairs; Purple line (no_CTCF), correlation between gene pairs not separated

689 by predicted CTCF sites.

690 Web links to original figures.

691 Figure 5. Schematic representation of chromatin interactions involving gene promoters

692 (Bailey et al. 2015).

693 https://www.nature.com/articles/ncomms7186/figures/5

694

695 **Figure 5.** Schematic representation of chromatin interactions involving gene promoters.

696 ZNF143 contributes the formation of chromatin interactions by directly binding the

697 promoter of genes establishing looping with distal element bound by CTCF (Bailey et al.

698 2015).

699

700

Tables

Table 1. Biased orientations of DNA binding motif sequences of TFs in monocytes, T cells, HMEC and NPC in common. TF: DNA binding motif sequences of transcription factors.

Forward-reverse orientation

TF	P-value
AHR	0
ARNT	0
ARNTL	7.96E-08
ATF2	3.09E-14
ATF3	2.22E-15
BCL	0
BHLHE41	5.55E-14
CREB3L1	0
CTCF	0
CXXC1	0
E2F	0
E2F1	0
EGR1	0
EGR3	0
EGR4	0
ELF1	0
ELF2	5.74E-13
ELK3	3.33E-15
ELK4	6.19E-11
ERG	0
ETS	0
ETS1	0
ETV7	2.31E-08
HEY2	0
HIC1	0
HINFP	6.46E-14
INSM1	2.22E-16
KLF4	0
KLF7	9.07E-09
MAX	0

TF	P-value
MYC	0
MYCN	0
MZF1	0
NFY	1.72E-11
NFYB	0
NONO	0
NRF1	1.63E-11
OVOL2	0
PLAG1	0
PLAGL1	0
RAD21	0
REST	0
RFX1	0
SIN3A	0
SIX5	0
SMC3	0
SP2	1.04E-11
TFAP2A	0
TFAP2B	2.22E-16
TFAP2C	0
TP73	0
USF1	0
XBP1	0
YY1	0
YY2	0
ZBTB33	0
ZBTB7A	0
ZFP62	0
ZFX	0
ZIC1	0

TF	P-value
ZNF143	0
ZNF740	0
ZNF770	6.51E-08
ZNF84	0

Reverse-forward orientation

TF	P-value
AP1	0
ARNT	1.26E-11
ATF3	0
BHLHE40	8.88E-16
CREB1	0
CTCF	0
E2F	2.32E-13
E2F3	0
EFNA2	6.61E-11
EGR1	0
EGR2	0
ETS1	0
FLI1	1.05E-13
FLI1:FIGLA	0
FOS	0
GMEB2	0
HIF1A	0
KLF4	0
MITF	0
MYB	0
MYC	0
MYCN	0
MZF1	0
NFKB1	0
NFYA	2.31E-13
NR3C1	0
NRF1	0
OSR2	0
PBX3	0
PLAG1	2.78E-14

TF	P-value
RFX2	0
RFX5	0
RUNX3	0
SP1	0
SP2	0
SP4	0
SPDEF	0
SREBF2	0
STAT	0
TATA	0
TFAP2B	2.00E-15
TFAP2C	0
TFCP2L1	0
USF1	7.55E-10
YBX1	0
YY1	0
YY2	0
ZBTB33	0
ZBTB7B	0
ZNF100	6.22E-14
ZNF143	0
ZNF432	0

709 **Table 2.** Comparison of enhancer-promoter interactions (EPIs) with chromatin
710 interactions in T cells. The upper tables show the number of biased orientations of DNA
711 motifs, where a significantly higher ratio of EPIs that were predicted based on an
712 enhancer-promoter association (EPA) (i) overlapped with HiChIP chromatin
713 interactions than the other types of EPA (ii) and (iii) in T cells. The middle tables show
714 133 FR and 90 RF orientations of DNA motifs found in common among B2T1, B2T2
715 and B3T1 replications in T cells in the upper table. The lower tables show that among
716 64 FR and 52 RF orientations of DNA motifs found in common in monocytes, T cell,
717 HMEC and NPC, 44 (69%) FR and 28 (54%) RF were matched with the analysis of
718 HiChIP chromatin interactions according to three types of EPAs. TF: DNA binding
719 motif sequence of a transcription factor. Score: $-\log_{10}$ (*p*-value). Score 1: Comparison of
720 an EPA shortened at the FR or RF orientation of DNA motif sites [EPA (i)] with an EPA
721 not shortened [EPA (iii)]. Score 2: Comparison of an EPA shortened at the FR or RF
722 orientation of DNA motif sites [EPA (i)] with an EPA shortened at the non-orientation of
723 DNA motif sites [EPA (ii)].

1. Comparison of EPI with HiChIP data among three EPA (i), (ii) and (iii)

Replication of HiChIP data	Total no. (FR + RF) of DNA motifs	No. of FR DNA motifs	No. of RF DNA motifs
B2T1	226	153	101
B2T2	221	149	98
B3T1	237	160	109
DNA motifs found in common among replications			
B2T1 and B2T2	212	141	95
B2T1 and B3T1	212	143	93
B2T2 and B3T1	208	138	93
B2T1, B2T2 and B3T1	201	133	90

2. Comparison of EPI with HiChIP data between two EPA (i) and (iii)

Replication of HiChIP data	Total no. (FR + RF) of DNA motifs	No. of FR DNA motifs	No. of RF DNA motifs
B2T1	395	262	205
B2T2	398	264	204
B3T1	394	263	203
DNA motifs found in common among replications			
B2T1 and B2T2	394	262	202
B2T1 and B3T1	391	261	202
B2T2 and B3T1	392	262	200
B2T1, B2T2 and B3T1	390	261	199

FR and RF orientations of DNA motifs found in common among three replications in T cell.

Forward-reverse (FR)

TF	Score 1	Score 2	TF	Score 1	Score 2	TF	Score 1	Score 2
AHR	38.81	13.41	ETS2	208.78	13.99	MNT	215.63	8.00
ARNTL	155.78	1.96	ETV1	153.32	7.02	MTF1	323.31	14.21
ATF1	323.31	15.00	ETV3	140.11	14.58	MXI1	323.31	70.98
ATF3	323.31	35.22	ETV5:EVX1	145.48	17.33	MYC	84.79	24.93
BCL	153.72	3.52	ETV5:HES7	8.76	8.74	MYCN	165.16	25.87
CREB	90.91	2.32	ETV5:TCF3	203.52	5.90	MZF1	81.83	2.29
CREB3	323.31	38.74	FOXN4	73.43	5.59	NFKB1	279.24	14.27
CREB3L1	323.31	27.96	FOXO1:ELK3	323.31	43.51	NFKB1:NFKB1	323.31	13.79
CTCF	323.31	3.50	GABPA	197.57	20.39	NFY	323.31	3.42
CTCFL	174.90	2.09	GABPA:GABPB1	142.28	6.10	NONO	323.31	9.24
CXXC1	69.92	3.30	GCM2	13.68	18.80	NR2C2	323.31	3.64
E2	323.31	20.15	GDNF	286.73	3.15	NRF1	45.13	30.75
E2F	122.12	21.87	GMEB1	136.68	10.56	OVOL2	323.31	31.61
E2F1	43.22	2.85	HIC1	223.55	4.56	PATZ1	101.85	9.30
EGR1	79.09	3.79	HIF1A	241.47	1.71	PLAG1	177.90	11.02
EGR2	176.69	4.53	HOXB2:ETV1	102.22	2.42	PURA	196.04	17.98
EGR3	85.25	34.18	ID2	323.31	14.52	R	22.49	3.99
EHF	323.31	8.66	INSM1	193.85	15.87	**RAD21**	258.21	4.81
ELF1	203.38	3.86	JUN:JUNB	275.78	6.48	RBAK	267.43	11.25
ELF2	227.62	7.83	JUNB:JUN	202.73	5.07	RELA	323.31	4.68
ELF5	323.31	8.76	KLF	252.10	8.35	RFX1	159.78	17.05
ELK1:TBX21	126.46	8.41	KLF15	323.31	22.56	RFX4	323.31	35.28
ELK1:TEF	323.31	7.99	KLF17	87.51	14.77	RFX5	323.31	26.52
ELK4	117.83	4.81	KLF2	90.74	15.34	SAP1	124.23	14.63
ENO1	80.42	3.13	KLF4	209.71	9.38	**SMC3**	222.09	1.76
EPAS1	65.43	7.76	KLF7	229.95	11.96	SP1	235.48	29.09
ERF	207.67	6.25	LHX8	244.38	2.95	SP2	94.11	9.54
ERG	199.81	25.70	MAX	323.31	8.35	SP4	14.30	6.31
ETS	196.80	1.63	MAZ	109.42	3.37	SPDEF	179.39	16.81
ETS1	308.00	3.92	MBD2	8.41	1.95	SPIC	323.31	28.49

TF	Score 1	Score 2
STAT	84.60	1.69
STAT1	323.31	5.38
TCF12	111.44	16.79
TCF3	323.31	14.05
TEAD4:ETV4	226.28	5.90
TFAP2A	25.86	20.26
TFAP2B	90.03	6.10
TFAP2C	169.60	8.55
TFAP4	93.98	2.36
TFE3	139.21	16.71
TP73	198.45	7.75
TR4	39.01	4.97
USF1	194.06	3.56
VEZF1	134.36	3.49
XBP1	323.31	44.58
XRCC5:XRCC6	132.56	3.92
YY1	62.59	5.30
ZBED6	183.14	20.23
ZBTB17	48.37	7.27
ZBTB26	151.91	16.84
ZBTB5	120.19	9.58
ZBTB7A	52.89	30.58
ZFX	13.33	14.55
ZFY	36.57	4.04
ZIC3	266.75	10.54
ZIC4	17.27	9.30
ZNF140	323.31	4.99
ZNF143	323.31	35.38
ZNF165	323.31	7.80
ZNF25	281.69	7.72

TF	Score 1	Score 2
ZNF322	120.49	11.55
ZNF325	69.42	2.74
ZNF408	214.73	2.22
ZNF467	127.21	4.64
ZNF479	226.76	3.26
ZNF48	106.17	9.88
ZNF511	84.74	9.87
ZNF553	93.45	9.17
ZNF555	232.83	7.63
ZNF624	235.50	3.84
ZNF672	266.64	10.80
ZNF675	323.31	5.81
ZNF676	323.31	16.54

Reverse-forward (RF)

TF	Score 1	Score 2
ARNT	323.31	14.12
ARNT2	41.41	42.78
ASCL2	138.15	6.41
ATF3	323.31	14.64
ATF4	323.31	25.14
ATF7	79.30	4.96
BCLAF1	148.24	8.52
BHLHE40	323.31	12.42
CDCA7L	84.72	8.42
CREB3	206.55	11.07
CREB3L1	323.31	7.63
CREB3L2	67.51	7.98
CTCF	240.61	4.56
E2F	78.16	7.07
E2F1	124.10	15.73
E2F3	65.67	8.85
E2F6	165.75	30.69
EFNA2	255.01	10.95
ELK3	143.48	7.57
EP300	121.01	10.90
ETV5:CLOCK	42.10	7.29
GLIS2	37.40	17.34
GMEB2	323.31	7.81
HES1	88.18	9.46
HES7	166.52	14.60
HIVEP1	323.31	4.90
HOXB2:ELK1	217.94	11.92
IRC900814	323.31	4.89
KLF4	213.35	9.49
KLF8	323.31	17.42

TF	Score 1	Score 2
MAX	304.34	8.64
MLXIPL	64.44	10.74
MUSCLE	23.05	3.47
MYB	323.31	17.68
MYBL1	316.23	23.27
MYC	323.31	12.23
MZF1	200.49	22.73
NFY	209.97	3.22
NFYA	323.31	11.75
NHLH1	105.19	4.42
NR1H3	323.31	9.38
NR3C1	43.16	8.31
OSR2	111.77	14.65
RFX1	323.31	22.99
RXRA	146.30	15.11
SALL1	277.84	1.91
SCRT2	301.48	9.60
SMAD6	259.24	7.43
SP100	20.75	7.99
SP2	294.86	2.59
SP4	110.94	19.63
SPDEF	185.85	14.35
SPZ1	323.31	9.87
SREBF1	67.27	15.74
SREBF2	297.27	1.62
TAF1	252.27	17.47
TATA	2.16	4.02
TFAP2A	20.17	29.15
TFAP2B	29.46	12.62
TFAP2C	112.10	51.21

TF	Score 1	Score 2
TFE3	95.23	10.59
THAP1	127.72	5.07
YY1	323.31	9.92
YY2	47.49	2.61
ZBTB33	90.29	7.78
ZBTB45	323.31	57.08
ZBTB7A	89.19	16.19
ZBTB7B	43.90	23.59
ZFP64	147.00	13.59
ZIC3	42.65	15.39
ZNF100	27.67	4.75
ZNF143	63.03	9.69
ZNF148	213.77	18.93
ZNF16	323.31	47.43
ZNF37A	310.67	14.79
ZNF410	140.45	13.57
ZNF419	247.63	11.25
ZNF429	87.05	32.39
ZNF436	323.31	11.48
ZNF468	21.12	7.67
ZNF557	299.44	9.58
ZNF575	39.45	14.38
ZNF586	260.73	6.18
ZNF611	279.80	15.65
ZNF616	189.53	30.98
ZNF692	202.47	2.33
ZNF727	214.01	17.22
ZNF770	300.52	4.71
ZNF773	150.45	8.84
ZSCAN21	323.31	5.55

FR and RF orientations of DNA motifs found in common in the four cell types.

Forward-reverse (FR)

TF	Score 1	Score 2
AHR	38.81	13.41
ARNTL	155.78	1.96
ATF3	323.31	35.22
BCL	153.72	3.52
CREB3L1	323.31	27.96
CTCF	323.31	3.50
CXXC1	69.92	3.30
E2F	122.12	21.87
E2F1	43.22	2.85
EGR1	79.09	3.79
EGR3	85.25	34.18
ELF1	203.38	3.86
ELF2	227.62	7.83
ELK4	117.83	4.81
ERG	199.81	25.70
ETS	196.80	1.63
ETS1	308.00	3.92
HIC1	223.55	4.56
INSM1	193.85	15.87
KLF4	209.71	9.38
KLF7	229.95	11.96
MAX	323.31	8.35
MYC	84.79	24.93
MYCN	165.16	25.87
MZF1	81.83	2.29
NFY	323.31	3.42
NONO	323.31	9.24
NRF1	45.13	30.75
OVOL2	323.31	31.61
PLAG1	177.90	11.02

TF	Score 1	Score 2
RAD21	258.21	4.81
RFX1	159.78	17.05
SMC3	222.09	1.76
SP2	94.11	9.54
TFAP2A	25.86	20.26
TFAP2B	90.03	6.10
TFAP2C	169.60	8.55
TP73	198.45	7.75
USF1	194.06	3.56
XBP1	323.31	44.58
YY1	62.59	5.30
ZBTB7A	52.89	30.58
ZFX	13.33	14.55
ZNF143	323.31	35.38

Reverse-forward (RF)

TF	Score 1	Score 2
ARNT	323.31	14.12
ATF3	323.31	14.64
BHLHE40	323.31	12.42
CTCF	240.61	4.56
E2F	78.16	7.07
E2F3	65.67	8.85
EFNA2	255.01	10.95
GMEB2	323.31	7.81
KLF4	213.35	9.49
MYB	323.31	17.68
MYC	323.31	12.23
MZF1	200.49	22.73
NFYA	323.31	11.75
NR3C1	43.16	8.31
OSR2	111.77	14.65
SP2	294.86	2.59
SP4	110.94	19.63
SPDEF	185.85	14.35
SREBF2	297.27	1.62
TATA	2.16	4.02
TFAP2B	29.46	12.62
TFAP2C	112.10	51.21
YY1	323.31	9.92
YY2	47.49	2.61
ZBTB33	90.29	7.78
ZBTB7B	43.90	23.59
ZNF100	27.67	4.75
ZNF143	63.03	9.69

Table 3. Correlation of expression level of gene pairs separated by DNA motif sites of a TF. Pairs of genes separated by 64 FR and 52 RF orientations of DNA motif sites of TFs found in common in monocytes, T cells, HMEC and NPC were analyzed to find significantly lower correlation of their expression level than the correlation of all pairs of nearby genes among 53 tissues. Score: $-\log_{10}$ (p-value) of Mann-Whitney test. Median correlation: median correlation coefficient of expression level of nearby gene pairs separated by DNA motif sites. The median correlation coefficient of expression level of all pairs of nearby genes is 0.17. # DNA site: number of DNA motif sites of a

TF separating gene pairs with expression data. All DNA motif sites of a TF were used, except for DNA motif sites separating pairs of ubiquitously expressed genes with coefficient of variance <90.

Forward-reverse (FR)

TF	Score	Median correlation	# DNA site
AHR	1.80	0.12	520
ARNT	1.35	0.09	141
ATF2	1.40	0.11	166
ATF3	3.61	0.11	795
BHLHE41	2.02	0.07	118
CREB3L1	2.88	0.05	127
CTCF	6.02	0.09	837
E2F	3.73	0.10	444
E2F1	3.79	0.11	868
EGR1	2.97	0.10	391
ELF1	4.86	0.10	714
ELF2	3.88	0.11	781
ELK3	1.86	0.12	547
ELK4	2.44	0.11	663
ETS	3.34	0.11	523
ETS1	4.27	0.11	687
ETV7	3.68	0.11	662
HIC1	1.65	0.11	380
HINFP	1.33	0.09	258
KLF4	2.00	0.13	718
MYC	3.86	0.11	762
MYCN	2.36	0.11	583
MZF1	1.74	0.10	261
NFYB	2.97	0.10	264
NRF1	2.21	0.11	640
PLAG1	2.93	0.10	503
PLAGL1	2.55	0.10	414
RAD21	6.08	0.09	852
REST	4.35	0.11	920
RFX1	2.38	0.08	81
SIN3A	3.31	0.11	813
SMC3	6.18	0.09	625
SP2	2.30	0.12	738
TFAP2A	4.17	0.11	767
TFAP2C	2.13	0.11	470
USF1	4.24	0.10	628
XBP1	6.65	0.07	379
ZBTB33	4.90	0.10	701
ZBTB7A	2.82	0.10	485
ZFP62	2.95	0.11	565
ZFX	2.69	0.11	581
ZIC1	4.47	0.11	829
ZNF770	3.38	0.08	271

Reverse-forward (RF)

TF	Score	Median correlation	# DNA site
AP1	3.87	0.11	744
ARNT	2.95	0.10	453
ATF3	4.34	0.10	665
BHLHE40	2.49	0.07	155
CREB1	1.79	0.11	303
CTCF	5.96	0.09	721
E2F	3.95	0.10	663
E2F3	4.05	0.09	616
EFNA2	3.51	0.10	543
EGR1	2.58	0.10	428
EGR2	1.39	0.13	747
ETS1	3.75	0.11	667
FLI1:FIGLA	5.41	0.08	428
FOS	3.51	0.11	777
GMEB2	1.36	0.09	310
HIF1A	2.34	0.11	448
KLF4	2.21	0.12	744
MITF	3.14	0.10	419
MYC	4.85	0.10	704
MYCN	2.79	0.10	507
NFKB1	1.59	0.11	342
NFYA	2.15	0.10	229
NRF1	2.01	0.12	615
OSR2	1.99	0.12	301
PBX3	2.20	0.11	253
RFX2	2.12	0.09	168
RFX5	3.03	0.05	75
RUNX3	2.01	0.11	241
SP1	2.73	0.11	725
SP2	2.15	0.12	1090
SP4	2.33	0.11	479
SPDEF	5.29	0.07	449
TFAP2B	3.42	0.11	855
TFAP2C	2.05	0.11	576
TFCP2L1	1.45	0.13	362
YBX1	1.34	0.13	160
YY1	2.23	0.01	50
ZBTB33	3.44	0.11	886
ZBTB7B	2.27	0.13	892
ZNF143	2.26	0.07	81

754 **Table 4.** Top 30 of co-location and overlapping biased orientations of DNA binding
755 motif sequences of TFs in monocytes. Co-location and overlapping DNA motif
756 sequences of CTCF with another biased orientation of DNA motif sequence are shown
757 in separate tables. Motif 1,2: DNA binding motif sequences of TFs. No.: the number of
758 genomic locations with both Motif 1 and Motif 2 in upstream and downstream of genes
759 in an EPA (< 1 Mb distance from TSS of genes). Total number of genes is 30,523.

760

761 Forward-reverse (FR)

Motif 1	Motif 2	No.	Mean of distances bet. DNA sites (nt)	Median of distances bet. DNA sites (nt)	Mean of distances from TSS (nt)	Median of distances from TSS (nt)	Interquartile range of distance from TSS (nt)
FOS	JUN	3332	0.00	0	43202.95	18085	5524 - 48583
CTCF	**SMC3**	2876	0.01	0	34606.92	13716	3073 - 39471
FOSL2	JUN	2807	0.00	0	40389.84	17365	5424 - 45251
FOSB	FOSL2	2644	0.00	0	44302.93	17867	5633 - 47209
EGR1	EGR2	2397	0.00	0	14578.21	1251	247 - 11473
CTCF	**RAD21**	2352	0.00	0	33492.68	12913	2824 - 37672
RAD21	**SMC3**	2343	0.02	0	33572.80	14302	3856 - 37159
ATF3	FOSL2	2322	0.00	0	42784.04	17841	5366 - 48236
FOSL2	JUNB	2305	0.02	0	42884.36	17867	5706 - 46515
ETS2	ETSLIKE	2205	0.00	0	37660.66	15765	4146 - 41462
FOS	JUNB	2151	0.00	0	38403.20	16367	4849 - 44736
IRF	IRF4	1962	0.00	0	40794.41	15872	3969 - 45946
FOSL2	SMARCC1	1945	0.00	0	42429.69	17369	5094 - 46586
EGR1	WT1	1941	0.16	0	12485.23	427	93 - 5394
FOSB	JUN	1808	0.02	0	36648.74	16705	5156 - 40309
ATF3	JUN	1713	0.02	0	38101.24	17119	5294 - 43559
JUN	TFAP2A	1628	0.00	0	42262.97	18017	5089 - 47094
FOSL2	TFAP2A	1628	0.00	0	36606.38	16201	4949 - 41948
BACH2	SMARCC1	1462	0.16	0	38673.02	14778	4060 - 41262
ELF1	ETS1	1459	0.00	0	37056.72	14346	3370 - 40339
CHD2	E2F	1429	0.00	0	19220.38	1579	329 - 16257
JUN	NR3C1	1262	0.00	0	35052.17	14418	3844 - 38534
USF1	USF2	1260	0.00	0	25188.91	4726	413 - 24699
BACH2	JUNB	1238	0.15	0	36252.37	15302	4462 - 39393
BACH2	FOSB	1184	0.22	0	37190.80	14778	4038 - 41262
ETSLIKE	GABPA	1164	0.00	0	32352.24	11683	2356 - 36919
CTCF	CTCFL	1151	0.00	0	30252.04	11606	2229 - 34539
NR5A1	NR5A2	1133	0.00	0	41171.86	12243	2488 - 43136
ATF3	BACH2	1094	0.18	0	35659.16	13605	3821 - 39756
ETS2	GABPA	1092	0.06	0	27250.24	12184	2858 - 32196

762

763

764

765

Reverse-forward (RF)

Motif 1	Motif 2	No.	Mean of distances bet. DNA sites (nt)	Median of distances bet. DNA sites (nt)	Mean of distances from TSS (nt)	Median of distances from TSS (nt)	Interquartile range of distance from TSS (nt)
EGR1	EGR3	3012	0.00	0	17005.00	709	149 - 10393
NR1I2	NR1I3	2932	0.00	0	49622.84	20548	5924 - 58436
ZIC1	ZIC3	2871	0.07	0	21511.64	3092	434 - 19128
EGR	WT1	2612	0.04	0	9949.38	396	102 - 4266
FOS	FOS:JUN	2512	0.01	0	37200.80	15466	4438 - 42373
EGR	EGR3	2293	0.17	0	11634.92	532	135 - 6044
MAFG	NFE2L1:MAFG	2272	0.03	0	34641.56	16917	5284 - 42097
KLF10	SP1	2233	0.00	0	9778.94	297	73 - 3077
EGR	EGR2	2160	0.16	0	10502.76	490	129 - 5227
KLF3	SP3	2036	0.00	0	6974.78	246	63 - 1447
KLF1	SP3	1771	0.00	0	7748.42	264	66 - 1829
KLF10	SP3	1734	0.00	0	7275.48	222	58 - 1320
KLF7	SP4	1639	0.00	0	12521.62	309	58 - 4894
KLF1	SP1	1574	0.05	0	6780.46	245	61 - 1438
AP1	JUNB	1572	0.05	0	34158.07	15451	4746 - 40315
EGR1	WT1	1543	0.31	0	12742.28	444	111 - 5553
EGR1	SP1:SP3	1393	0.08	0	7789.54	307	91 - 1886
FOS:JUN	JUNB	1386	0.14	0	33012.80	14245	3900 - 37988
SP1	SP3	1372	0.00	0	8845.31	293	77 - 1816
EHF	ELF1	1366	0.02	0	41217.39	13357	2842 - 43178
CTCF	RXRA	1362	0.00	0	29981.33	10937	2100 - 31407
AP1	FOS	1327	0.03	0	33225.52	13455	3503 - 37399
ATF1	ATF3	1215	0.00	0	23125.06	3798	342 - 21091
ELK1	ZNF200	1156	0.05	0	22200.49	2883	181 - 17610
SP1	SP4	1137	0.00	0	7371.85	215	63 - 1232
EHF	ELF3	1134	0.00	0	36296.46	10912	596 - 37318
MEIS2	TGIF1	1018	0.00	0	47677.15	17654	3273 - 49233
KLF3	SP1	1017	0.06	0	6514.33	226	60 - 994
SPI1	ZNF200	913	0.06	0	10962.81	425	85 - 6046
AP1	FOS:JUN	860	0.09	0	50412.92	24217	7302 - 60018

Co-location and overlapping DNA motifs of CTCF with another DNA motifs.

FR orientation of CTCF

Motif 1	Motif 2	No.	Mean of distances bet. DNA sites (nt)	Median of distances bet. DNA sites (nt)	Mean of distances from TSS (nt)	Median of distances from TSS (nt)	Interquartile range of distance from TSS (nt)
CTCF	SMC3	2876	0.01	0	34606.92	13716	3073 - 39471
CTCF	RAD21	2352	0.00	0	33492.68	12913	2824 - 37672
CTCF	CTCFL	1151	0.00	0	30252.04	11606	2229 - 34539
CTCF	ZBTB7A	470	0.27	0	23227.96	7065	745 - 23496
CTCF	E2F	123	0.81	0	7913.36	222	61 - 1997
CTCF	WT1	120	0.00	0	3543.72	114	44 - 375
CTCF	MYC	110	2.30	0	31289.45	11948	2887 - 33972

RF orientation of CTCF

Motif 1	Motif 2	No.	Mean of distances bet. DNA sites (nt)	Median of distances bet. DNA sites (nt)	Mean of distances from TSS (nt)	Median of distances from TSS (nt)	Interquartile range of distance from TSS (nt)
CTCF	RXRA	1362	0.00	0	29981.33	10937	2100 - 31407
CTCF	CTCFL	429	0.00	0	25171.22	9834	1859 - 24741
CTCF	RAD21	337	0.00	0	38829.91	17973	6117 - 45749
CTCF	ZIC1	126	1.40	0	35480.65	10286	2316 - 29380
CTCF	ZIC3	108	0.00	0	30219.32	10904	4463 - 31037

775

776 **References**

777

778 Ackerman SL, Minden AG, Williams GT, Bobonis C, Yeung CY. 1991. Functional
779 significance of an overlapping consensus binding motif for Sp1 and Zif268 in
780 the murine adenosine deaminase gene promoter. *Proc Natl Acad Sci U S A* **88**:
781 7523-7527.

782 Ansari AZ, Peterson-Kaufman KJ. 2011. A partner evokes latent differences between
783 Hox proteins. *Cell* **147**: 1220-1221.

784 Bailey SD, Zhang X, Desai K, Aid M, Corradin O, Cowper-Sal Lari R, Akhtar-Zaidi B,
785 Scacheri PC, Haibe-Kains B, Lupien M. 2015. ZNF143 provides sequence
786 specificity to secure chromatin interactions at gene promoters. *Nat Commun* **2**:
787 6186.

788 Barutcu AR, Lajoie BR, Fritz AJ, McCord RP, Nickerson JA, van Wijnen AJ, Lian JB,
789 Stein JL, Dekker J, Stein GS et al. 2016. SMARCA4 regulates gene expression
790 and higher-order chromatin structure in proliferating mammary epithelial cells.
791 *Genome research* **26**: 1188-1201.

792 Chatterjee R, Zhao J, He X, Shlyakhtenko A, Mann I, Waterfall JJ, Meltzer P,
793 Sathyanarayana BK, FitzGerald PC, Vinson C. 2012. Overlapping ETS and CRE
794 Motifs ((G/C)CGGAAGTGACGTCA) preferentially bound by GABPalpha and
795 CREB proteins. *G3 (Bethesda)* **2**: 1243-1256.

796 Chen M, Manley JL. 2009. Mechanisms of alternative splicing regulation: insights from
797 molecular and genomics approaches. *Nat Rev Mol Cell Biol* **10**: 741-754.

798 Das D, Clark TA, Schweitzer A, Yamamoto M, Marr H, Arribere J, Minovitsky S,
799 Poliakov A, Dubchak I, Blume JE et al. 2007. A correlation with exon
800 expression approach to identify cis-regulatory elements for tissue-specific
801 alternative splicing. *Nucleic acids research* **35**: 4845-4857.

802 de Wit E, Vos ES, Holwerda SJ, Valdes-Quezada C, Verstegen MJ, Teunissen H,
803 Splinter E, Wijchers PJ, Krijger PH, de Laat W. 2015. CTCF Binding Polarity
804 Determines Chromatin Looping. *Molecular cell* **60**: 676-684.

805 Guo Y, Xu Q, Canzio D, Shou J, Li J, Gorkin DU, Jung I, Wu H, Zhai Y, Tang Y et al.
806 2015. CRISPR Inversion of CTCF Sites Alters Genome Topology and

807 Enhancer/Promoter Function. *Cell* **162**: 900-910.
808 He X, Syed KS, Tillo D, Mann I, Weirauch MT, Vinson C. 2015. GABPalpha Binding
809 to Overlapping ETS and CRE DNA Motifs Is Enhanced by CREB1: Custom
810 DNA Microarrays. *G3 (Bethesda)* **5**: 1909-1918.
811 Hsu SC, Gilgenast TG, Bartman CR, Edwards CR, Stonestrom AJ, Huang P, Emerson
812 DJ, Evans P, Werner MT, Keller CA et al. 2017. The BET Protein BRD2
813 Cooperates with CTCF to Enforce Transcriptional and Architectural Boundaries.
814 *Molecular cell* **66**: 102-116 e107.
815 Jolma A, Yan J, Whitington T, Toivonen J, Nitta KR, Rastas P, Morgunova E, Enge M,
816 Taipale M, Wei G et al. 2013. DNA-binding specificities of human transcription
817 factors. *Cell* **152**: 327-339.
818 Jolma A, Yin Y, Nitta KR, Dave K, Popov A, Taipale M, Enge M, Kivioja T, Morgunova
819 E, Taipale J. 2015. DNA-dependent formation of transcription factor pairs alters
820 their binding specificity. *Nature* **527**: 384-388.
821 Jung I, Schmitt A, Diao Y, Lee AJ, Liu T, Yang D, Tan C, Eom J, Chan M, Chee S et al.
822 2019. A compendium of promoter-centered long-range chromatin interactions in
823 the human genome. *Nature genetics* **51**: 1442-1449.
824 Karolchik D, Barber GP, Casper J, Clawson H, Cline MS, Diekhans M, Dreszer TR,
825 Fujita PA, Guruvadoo L, Haeussler M et al. 2014. The UCSC Genome Browser
826 database: 2014 update. *Nucleic acids research* **42**: D764-770.
827 Katainen R, Dave K, Pitkanen E, Palin K, Kivioja T, Valimaki N, Gylfe AE, Ristolainen
828 H, Hanninen UA, Cajuso T et al. 2015. CTCF/cohesin-binding sites are
829 frequently mutated in cancer. *Nature genetics* **47**: 818-821.
830 Kel AE, Gossling E, Reuter I, Cheremushkin E, Kel-Margoulis OV, Wingender E. 2003.
831 MATCH: A tool for searching transcription factor binding sites in DNA
832 sequences. *Nucleic acids research* **31**: 3576-3579.
833 Kheradpour P, Kellis M. 2014. Systematic discovery and characterization of regulatory
834 motifs in ENCODE TF binding experiments. *Nucleic acids research* **42**:
835 2976-2987.
836 Kin K, Chen X, Gonzalez-Garay M, Fakhouri WD. 2016. The effect of non-coding
837 DNA variations on P53 and cMYC competitive inhibition at cis-overlapping
838 motifs. *Hum Mol Genet* **25**: 1517-1527.
839 Kulakovskiy IV, Vorontsov IE, Yevshin IS, Sharipov RN, Fedorova AD, Rumynskiy EI,

840 Medvedeva YA, Magana-Mora A, Bajic VB, Papatsenko DA et al. 2018.
841 HOCOMOCO: towards a complete collection of transcription factor binding
842 models for human and mouse via large-scale ChIP-Seq analysis. *Nucleic acids*
843 *research* **46**: D252-D259.
844 Li H, Durbin R. 2009. Fast and accurate short read alignment with Burrows-Wheeler
845 transform. *Bioinformatics (Oxford, England)* **25**: 1754-1760.
846 Lieberman-Aiden E, van Berkum NL, Williams L, Imakaev M, Ragoczy T, Telling A,
847 Amit I, Lajoie BR, Sabo PJ, Dorschner MO et al. 2009. Comprehensive
848 mapping of long-range interactions reveals folding principles of the human
849 genome. *Science (New York, NY)* **326**: 289-293.
850 McLean CY, Bristor D, Hiller M, Clarke SL, Schaar BT, Lowe CB, Wenger AM,
851 Bejerano G. 2010. GREAT improves functional interpretation of cis-regulatory
852 regions. *Nature biotechnology* **28**: 495-501.
853 Merabet S, Mann RS. 2016. To Be Specific or Not: The Critical Relationship Between
854 Hox And TALE Proteins. *Trends Genet* **32**: 334-347.
855 Mumbach MR, Satpathy AT, Boyle EA, Dai C, Gowen BG, Cho SW, Nguyen ML,
856 Rubin AJ, Granja JM, Kazane KR et al. 2017. Enhancer connectome in primary
857 human cells identifies target genes of disease-associated DNA elements. *Nature*
858 *genetics* **49**: 1602-1612.
859 Neph S, Kuehn MS, Reynolds AP, Haugen E, Thurman RE, Johnson AK, Rynes E,
860 Maurano MT, Vierstra J, Thomas S et al. 2012. BEDOPS: high-performance
861 genomic feature operations. *Bioinformatics (Oxford, England)* **28**: 1919-1920.
862 Newburger DE, Bulyk ML. 2009. UniPROBE: an online database of protein binding
863 microarray data on protein-DNA interactions. *Nucleic acids research* **37**:
864 D77-82.
865 Osato N. 2018. Characteristics of functional enrichment and gene expression level of
866 human putative transcriptional target genes. *BMC Genomics* **19**: 957.
867 Portales-Casamar E, Thongjuea S, Kwon AT, Arenillas D, Zhao X, Valen E, Yusuf D,
868 Lenhard B, Wasserman WW, Sandelin A. 2010. JASPAR 2010: the greatly
869 expanded open-access database of transcription factor binding profiles. *Nucleic*
870 *acids research* **38**: D105-110.
871 Purmann A, Toedling J, Schueler M, Carninci P, Lehrach H, Hayashizaki Y, Huber W,
872 Sperling S. 2007. Genomic organization of transcriptomes in mammals:

873 Coregulation and cofunctionality. *Genomics* **89**: 580-587.
874 Rao SS, Huntley MH, Durand NC, Stamenova EK, Bochkov ID, Robinson JT, Sanborn
875 AL, Machol I, Omer AD, Lander ES et al. 2014. A 3D map of the human
876 genome at kilobase resolution reveals principles of chromatin looping. *Cell* **159**:
877 1665-1680.
878 Schreiber J, Libbrecht M, Bilmes J, Noble W. 2017. Nucleotide sequence and DNaseI
879 sensitivity are predictive of 3D chromatin architecture. *bioRxiv*.
880 Sherwood RI, Hashimoto T, O'Donnell CW, Lewis S, Barkal AA, van Hoff JP, Karun V,
881 Jaakkola T, Gifford DK. 2014. Discovery of directional and nondirectional
882 pioneer transcription factors by modeling DNase profile magnitude and shape.
883 *Nature biotechnology* **32**: 171-178.
884 Shlyueva D, Stampfel G, Stark A. 2014. Transcriptional enhancers: from properties to
885 genome-wide predictions. *Nature reviews Genetics* **15**: 272-286.
886 Shrivastava A, Calame K. 1994. An analysis of genes regulated by the multi-functional
887 transcriptional regulator Yin Yang-1. *Nucleic acids research* **22**: 5151-5155.
888 Slattery M, Riley T, Liu P, Abe N, Gomez-Alcala P, Dror I, Zhou T, Rohs R, Honig B,
889 Bussemaker HJ et al. 2011. Cofactor binding evokes latent differences in DNA
890 binding specificity between Hox proteins. *Cell* **147**: 1270-1282.
891 Tabuchi TM, Deplancke B, Osato N, Zhu LJ, Barrasa MI, Harrison MM, Horvitz HR,
892 Walhout AJ, Hagstrom KA. 2011. Chromosome-biased binding and gene
893 regulation by the Caenorhabditis elegans DRM complex. *PLoS Genet* **7**:
894 e1002074.
895 van Helden J. 2003. Regulatory sequence analysis tools. *Nucleic acids research* **31**:
896 3593-3596.
897 Wang ET, Sandberg R, Luo S, Khrebtukova I, Zhang L, Mayr C, Kingsmore SF,
898 Schroth GP, Burge CB. 2008. Alternative isoform regulation in human tissue
899 transcriptomes. *Nature* **456**: 470-476.
900 Wang J, Vicente-Garcia C, Seruggia D, Molto E, Fernandez-Minan A, Neto A, Lee E,
901 Gomez-Skarmeta JL, Montoliu L, Lunyak VV et al. 2015. MIR retrotransposon
902 sequences provide insulators to the human genome. *Proc Natl Acad Sci U S A*
903 **112**: E4428-4437.
904 Wang J, Zhuang J, Iyer S, Lin X, Whitfield TW, Greven MC, Pierce BG, Dong X,
905 Kundaje A, Cheng Y et al. 2012a. Sequence features and chromatin structure

906 around the genomic regions bound by 119 human transcription factors. *Genome*
907 *research* **22**: 1798-1812.
908 Wang L, Wang S, Li W. 2012b. RSeQC: quality control of RNA-seq experiments.
909 *Bioinformatics (Oxford, England)* **28**: 2184-2185.
910 Wei Z, Gao F, Kim S, Yang H, Lyu J, An W, Wang K, Lu W. 2013. Klf4 organizes
911 long-range chromosomal interactions with the oct4 locus in reprogramming and
912 pluripotency. *Cell Stem Cell* **13**: 36-47.
913 Weintraub AS, Li CH, Zamudio AV, Sigova AA, Hannett NM, Day DS, Abraham BJ,
914 Cohen MA, Nabet B, Buckley DL et al. 2017. YY1 Is a Structural Regulator of
915 Enhancer-Promoter Loops. *Cell* **171**: 1573-1588 e1528.
916 Wingender E, Dietze P, Karas H, Knuppel R. 1996. TRANSFAC: a database on
917 transcription factors and their DNA binding sites. *Nucleic acids research* **24**:
918 238-241.
919 Xi H, Yu Y, Fu Y, Foley J, Halees A, Weng Z. 2007. Analysis of overrepresented motifs
920 in human core promoters reveals dual regulatory roles of YY1. *Genome research*
921 **17**: 798-806.
922 Xie X, Lu J, Kulbokas EJ, Golub TR, Mootha V, Lindblad-Toh K, Lander ES, Kellis M.
923 2005. Systematic discovery of regulatory motifs in human promoters and 3'
924 UTRs by comparison of several mammals. *Nature* **434**: 338-345.
925 Xie X, Mikkelsen TS, Gnirke A, Lindblad-Toh K, Kellis M, Lander ES. 2007.
926 Systematic discovery of regulatory motifs in conserved regions of the human
927 genome, including thousands of CTCF insulator sites. *Proc Natl Acad Sci U S A*
928 **104**: 7145-7150.
929 Xie Z, Hu S, Blackshaw S, Zhu H, Qian J. 2010. hPDI: a database of experimental
930 human protein-DNA interactions. *Bioinformatics (Oxford, England)* **26**:
931 287-289.
932 Yardimci GG, Ozadam H, Sauria MEG, Ursu O, Yan KK, Yang T, Chakraborty A, Kaul
933 A, Lajoie BR, Song F et al. 2019. Measuring the reproducibility and quality of
934 Hi-C data. *Genome Biol* **20**: 57.
935 Yoon SO, Chikaraishi DM. 1992. Tissue-specific transcription of the rat tyrosine
936 hydroxylase gene requires synergy between an AP-1 motif and an overlapping E
937 box-containing dyad. *Neuron* **9**: 55-67.
938 Zhang H, Li F, Jia Y, Xu B, Zhang Y, Li X, Zhang Z. 2017. Characteristic arrangement

939 of nucleosomes is predictive of chromatin interactions at kilobase resolution.
940 *Nucleic acids research* **45**: 12739-12751.
941 Zhang Y, Liu T, Meyer CA, Eeckhoute J, Johnson DS, Bernstein BE, Nusbaum C,
942 Myers RM, Brown M, Li W et al. 2008. Model-based analysis of ChIP-Seq
943 (MACS). *Genome Biol* **9**: R137.
944 Zhao Y, Stormo GD. 2011. Quantitative analysis demonstrates most transcription factors
945 require only simple models of specificity. *Nature biotechnology* **29**: 480-483.
946